Climate change impacts on floods in West Africa: New insight from two large-scale hydrological models

Serigne Bassirou Diop 1
Job Ekolu 2
Yves Tramblay 3
Bastien Dieppois 2
Stefania Grimaldi 4
Ansoumana Bodian 1
Juliette Blanchet 5
Ponnambalam Rameshwaran 6
Peter Salamon 4
Benjamin Sultan 3

1 Laboratoire Leïdi "Dynamique des Territoires et Développement", Université Gaston Berger, Saint-Louis, Senegal

2 Centre for Agroecology, Water and Resilience, Coventry University, Coventry, UK

3 Espace-Dev, Univ. Montpellier, IRD, Montpellier, France

4 European Commission, Joint Research Centre (JRC), Ispra, Italy

5 Univ. Grenoble Alpes, CNRS, IRD, Grenoble INP, IGE, Grenoble, France

6 UK Centre for Ecology & Hydrology, Wallingford, UK

Correspondence to: Serigne Bassirou Diop (09.bachir.diop.10@gmail.com)

Abstract

West Africa is projected to face unprecedented shifts in temperature and extreme precipitation patterns as a result of climate change. The devastating impacts of river flooding are already being felt in most West African countries, emphasizing the urgent need for comprehensive insights into the frequency and magnitude of floods to guide the design of hydraulic infrastructure for effective flood risk mitigation and water resource management. Despite its significant socio-economic and environmental impacts, flood hazards remain poorly documented in West Africa due to the data-related challenges. This study aims to fill this knowledge gap by providing a large-scale analysis of flood frequency and magnitudes across West Africa, focusing on how climate change may influence future flood trends. To achieve this, we have used two large-scale hydrological models driven by five bias-corrected CMIP6 climate models under two Shared Socioeconomic Pathways (SSPs). The Generalized Extreme Value (GEV) distribution was utilized to analyze trends and detect change points by comparing multiple non-stationary GEV models across historical and future periods for a set of 58 catchments. Both hydrological models consistently projected increases in flood frequency and magnitude across West Africa, despite their differences in hydrological processes representation and calibration schemes. ~~Flood magnitude is projected to increase for 94 % of the stations, with some locations experiencing increases exceeding 45 % in magnitude. In addition, the majority of trends are starting from the historical period, under both SSP2-4.5 and SSP5-8.5.~~Flood magnitudes are projected to increase at 94% (96%) of stations for the 2-year (20-year) event in the near-term future, and at 88% (93%) of stations for the 2-year (20-year) event in the long-term future, with some locations expected to experience increases exceeding 45%. The findings from this study provide regional-scale insights into the evolving flood risks across West Africa and highlight the urgent need for climate-resilient strategies to safeguard populations and infrastructure against the increasing threat of flood hazards.

Keywords: Flood frequency analysis, GEV, GMLE, West Africa, climate change, CMIP, SSP

1 Introduction

Anthropogenic changes in atmospheric composition and land use have led to climate change (Houghton et al., 2001; Hansen et al., 2010; Santer et al., 2019; Masson-Delmotte et al., 2021). Climate change, in turn, amplifies the frequency, intensity, and impact of extreme events, such as heatwaves, storms, floods, and droughts at the global scale (IPCC, 2021). West Africa is identified as a hotspot for climate change impacts, as the region is projected to experience unprecedented shifts in both temperature and extreme precipitation patterns (IPCC, 2021). West African populations are therefore becoming increasingly vulnerable for floods and droughts (Tramblay et al., 2020, Rameshwaran et al., 2021). This vulnerability is due to multiple factors such as the region's reliance on rainfed agriculture and the dependence of its rural communities on the natural environment (Krishnamurthy et al., 2012; Totin et al., 2016; Land et al., 2018; Diallo et al., 2020; De Longueville et al., 2020; Matthew et al., 2020). Additionally, the limited economic and institutional resources available to manage and adapt to climate change and natural hazards exacerbate this vulnerability (Roudier et al., 2011; Sultan & Gaetani, 2016; Lalou et al., 2019).

A potential increase in river flooding risks is one of the most frequently studied impacts of climate change (Arnell & Gosling, 2016), because of the devastating economic and environmental impacts it may trigger (EM-DAT, 2015; CRED, 2022; UNDRR, 2023). Such impacts of climate change are already being felt in many West African countries, which experienced several catastrophic floods in the past few years, raising concerns for water management and livelihoods (World Bank, 2021a). It is therefore becoming crucial to develop efficient adaptation strategies for mitigating the adverse effects of flood hazards on West African communities and economies.

Efficient water resources management is essential for sustainable development in West Africa in a changing climate (UNEP, 2020). However, water management requires comprehensive insights into the frequency and magnitude of floods to design appropriate hydraulic infrastructure (Feaster et al., 2023), and quantification of watershed runoff to design reservoirs for agricultural, industrial, and municipal water use (Song et al., 2022). In West Africa however, access to hydrometric data remains a challenge, as the number of stations within hydro-monitoring networks has decreased in recent years (Bodian et al., 2020; Tarpanelli et al., 2023). Existing hydrometric databases, available to estimate design flows, only provide short and often old records (Agoungbome et al., 2018; Tramblay et al., 2021). ~~Therefore, updating these~~

~~hydrological standards is essential to ensure that they accurately represent the current hydroclimatic context of the region (Wasko et al., 2021).~~Therefore, updating these design flood estimation values (i.e. used to build dams or reservoirs) is essential to ensure that they accurately represent the current hydroclimatic context of the region (Wasko et al., 2021)

Global Climate Models (GCMs) outputs from the fifth/sixth Coupled Model Intercomparison Project (CMIP5/6), which contributed to the fifth and sixth Assessment Report (AR5/6) of the Intergovernmental Panel on Climate Change (IPCC), have provided opportunities to simulate future hydrological impacts of climate change worldwide. Indeed, CMIP5/6 models use a range of scenarios that represent different future trajectories to simulate several climate variables, which help researchers assess the potential long-term impacts of near-term decisions on emissions reductions and climate policies (Riahi et al., 2017). To understand future trends in hydrological extremes, climate models are typically used in combination with hydrological modelling experiments. However, the simulations from GCMs cannot be used directly to drive hydrological models as they are associated with systematic biases relative to observational datasets (Sillmann et al., 2013). Therefore, downscaling and bias-correction algorithms are routinely applied to leverage the information from GCM outputs (Ehret et al., 2012). ~~Nevertheless, large uncertainties remain regarding future climate trends in West Africa, due to the sensitivity of different climate models contrasting warming in the North Atlantic and Mediterranean Sea, which are known to influence the West African Monsoon (Bichet et al., 2020; Monerie et al., 2023), and due to contrasting emission scenarios (IPCC, 2021).~~Nevertheless, large uncertainties remain regarding future climate trends in West Africa, partly due to differences in how climate models simulate projected warming of the North Atlantic and Mediterranean Sea, affecting the West African Monsoon and projected rainfall changes in the region (Bichet et al., 2020; IPCC, 2021; Monerie et al., 2023).

As climate change may intensify the hydrological cycle (Gudmundsson et al., 2012), systematically assessing future flood risks and regional-scale hydrological impacts of future climate change is crucial for developing effective climate adaptation strategies (Huang et al., 2024). Due to their simplicity and computational efficiency, lumped hydrological models have been widely applied in West Africa (Niel et al., 2003; Bodian et al., 2016; 2018; Kwakye & Bárdossy, 2020; Koubodana et al., 2021). However, because runoff generation is an inherently spatial and temporally dynamic process, changing environmental conditions may impact flood frequencies and water availability (Wilson et al., 1979; Haddeland et al., 2002; Descroix et al.,

2018). Although lumped models often perform comparably or even better than distributed models at the catchment outlet (Reed et al., 2004), their main limitation lies in evaluating the overall catchment response simply at the outlet, without accounting for the contributions of upstream individual sub-basins (Cunderlik, 2003; Pokhrel et al., 2008; Jajarmizad et al., 2012). The main advantage of distributed models is not necessarily a higher accuracy of runoff simulations at specific points (e.g., outlet or gauge stations), but rather their broader applicability and ability to simulate the impacts of spatially varying drivers and scenarios (Gebremeskel et al., 2005; Tang et al., 2007; Thielen et al., 2009; Chu et al., 2010; Tran et al., 2018). The interest in large-scale hydrological models has increased due to the need to sustainably manage large river basins and the pervasive global environmental change (Döll et al., 2008). As global hydrological models can capture the variability of hydrological processes across different geographical and climatic contexts, large-scale hydrological modelling has become a key tool for analysing global and regional water resources, assessing climate impacts, and managing water resources (Kauffeldt et al., 2013; Prudhomme et al., 2024). However, running physically based large-scale hydrological models requires numerous input variables that describe the physiographic characteristics of the watersheds (such as soil moisture, land use/land cover, topography, etc.), along with several meteorological forcings. Thus, this complexity limits the widespread use of these models. Brunner et al. (2021) have argued that the limited information on regional flood trends is partly due to the data-related challenges. In the West African context, several studies have shown the increase in extreme rainfall in observations (Taylor et al., 2017, Tramblay et al., 2020, Chagnaud et al., 2022) and future climate scenarios (Dosio et al., 2021, Chagnaud et al., 2023), but very few studies have used GCMs simulations as forcings to drive grid-based large-scale hydrological models to assess the potential impacts of climate change on river flows across West Africa (Rameshwaran et al., 2021; Ekolu et al., 2024, https://africa-hydrology.ceh.ac.uk/). The main objective of this study is to address this gap by assessing the impacts of climate change on floods in the West African region from two large-scale hydrological models driven by data from five bias-corrected CMIP6 GCMs under two Shared Socioeconomic Pathways (SSPs; O'Neill et al., 2017). This article is organised as follows: In Section 2, we describe the study area. Section 3 outlines the materials and methods, including the data used in the analysis, the CMIP6 models and hydrological modelling approach, the non-stationary extreme value analysis framework, and the evaluation of climate change impacts on floods at both local and regional scales. In Section 4, we present and discuss the findings. Finally, main conclusions and perspectives are given in Section 5.

2 Materials and Methods

2.1 Study area description

West Africa covers about one-fifth of the African continent, extending from the Atlantic coast of Senegal (18°W) to eastern Chad (25°E) and from the Gulf of Guinea (4°N) to the Sahel (25°N) (Figure 1). The region's climate is governed by the Inter-Tropical Convergence Zone (ITCZ) or the Inter-Tropical Discontinuity (ITD), which represents the interface at the ground between moist monsoon air and dry harmattan air with a migratory annual cycle (Pospichal et al., 2010). The West African region features high climatic diversity (Vintrou, 2012), and covers a wide range of ecosystems and bioclimatic regions (Nicholson, 2018). The latitudinal and seasonal oscillation of the ~~Inter-ITCZ~~ITCZ divides the region into three main climatic domains, namely the Sahel, Sudanian and Guinean zones (Sule & Odekunle, 2016). The Sahel zone is a semi-arid region with a short rainy season and an annual average rainfall not exceeding 600 mm (Figure 1). This domain is highly vulnerable to the adverse effects of climate change (Tian et al., 2023). The Sudanian zone stretches as a broad belt south of the Sahel, receiving an average rainfall of 600 to 1200 mm (Srivast et al., 2023). The Guinean zone, known for its rugged terrain with steep slopes (Orange, 1990), receives abundant rainfall throughout the year, with an annual average between 1200 and 2200 mm (ECOWREX, 2018). These three climate zones are characterized by distinct vegetation (Biaou et al., 2023) and rainy season patterns. The Sahelian and Sudanian domains share a unimodal rainfall pattern, while the Guinean zone experiences a bimodal rainfall pattern of two rainy seasons, driven by the West African Monsoon (Rodríguez-Fonseca et al., 2015; Nicholson, 2018). ~~It is worth noting that nearly half of Africa's continental watersheds are located in West Africa.~~It is worth noting that nearly half of African watersheds are located in West Africa. The socioeconomic development (agriculture, energy production, and livelihoods) of the region relies highly on the water resources provided by these transboundary basins and aquifers (World Bank, 2021b).

~~2.2 Observational data~~

2.2 Observational data and climate forcings for hydrological experiments

a mis en forme : Police :14 pt, Gras

~~Daily streamflow data for the period 1950-2018 were obtained from the African Database of Hydrometric Indices (Tramblay et al. 2021b, Diop et al., 2025). This database provides hydrometric indices computed from different data sources, with daily discharge time series that span at least 10 years. In the ADHI database, the size of the 441 West African catchments ranges from 95 to 2,150,000 km^2, and some stations have daily discharge data spanning over 44 years. Figure 1 shows the spatial distribution of the ADHI stations used in this study. We only selected watersheds that met the following three criteria: (i) low regulation (see Supplementary Figure S1), (ii) surface area of less than 150,000 km^2, and (iii) a daily streamflow time series covering a minimum of 10 years between the 1950 and 2018.~~ Daily streamflow data for the period 1950-2018 were obtained from the African Database of Hydrometric Indices (ADHI) recently developed by Tramblay et al. (2021). This database provides hydrometric indices computed from different data sources, with daily discharge time series that span at least 10 years. In the ADHI database, the size of the 441 West African catchments ranges from 95 to 2,150,000 km2, and some stations have daily discharge data spanning over 44 years. Figure 1 shows the spatial distribution of the ADHI stations used in this study, and Supplementary Table S1 gives information on their geographical locations (longitude and latitude), catchment areas, mean annual catchment-averaged rainfall, mean annual streamflow, and the range of years over which streamflow data is available. We only selected watersheds from the ADHI database that met the following three criteria: (i) low regulation, determined through visual inspection of dam locations relative to watershed outlets (see Supplementary Figure S1), combined with a year-by-year analysis of annual hydrographs to assess the impact of dam operations on streamflow, (ii) surface area of less than 150,000 km^2, and (iii) a daily streamflow time series covering a minimum of 10 years between the 1950 and 2018. To address the challenges associated with missing data in the database, we conducted a visual inspection of hydrographs at each station as illustrated by Supplementary Figure S2. Years with data gaps near the flood peak were excluded from the analysis to avoid the risk of missing the true annual peak flood (Wilcox et al., 2018). Through this careful screening process, we ensured that no AMF values were derived from periods characterized by a lot of missing data. It is important to note that the observational streamflow data are not used to calibrate or drive the hydrological models. Instead, these observations serve as an independent benchmark to evaluate the ability of the hydrological models to reproduce key flood statistics during the historical period. The LISFLOOD model was calibrated using the ERA5 reanalysis dataset, which provides consistent and high-resolution precipitation and temperature fields. Moreover, ERA5 was also used as a reference for the bias correction of the five climate models

from the CMIP6 ensemble that were used to drive the hydrological simulations for both the historical and future periods (see Section 2.4).

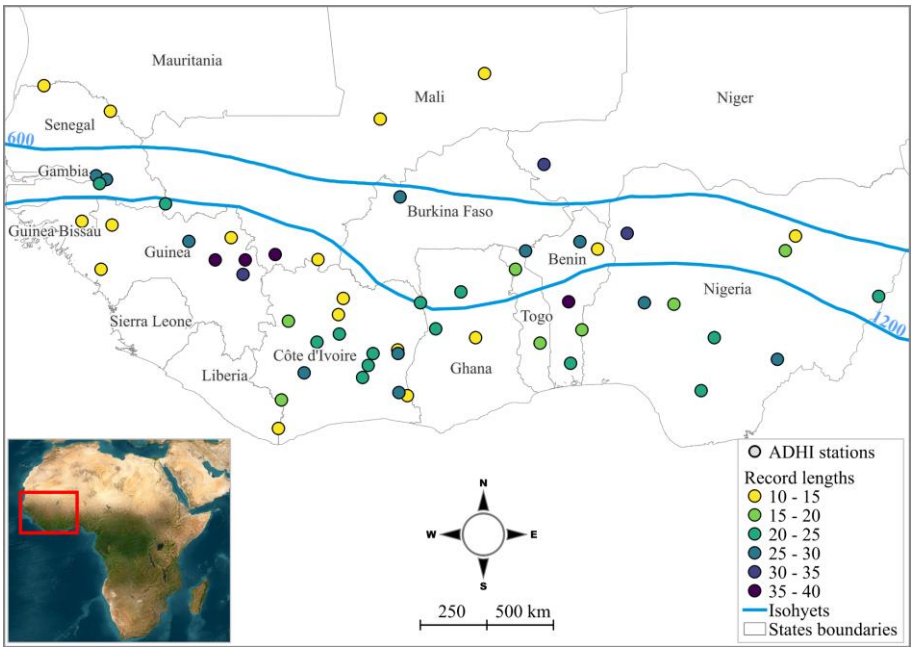

Figure 1: Spatial distribution of the stations used in this study, covering the three climatic zones in the West African region, as delimited by the blue isohyets (600 mm and 1200 mm annual rainfall) on the map. The color of the circles indicates the record lengths of flood data (in years). The blue lines represent isohyets delimiting West African climatic regions, and the ~~white~~grey lines indicate the borders of West African countries (African map from NASA 2005).

2.3 hydrological models

Two grid-based large-scale hydrological models were used to simulate river flows for the period from 1950 to 2010: the HMF-WA model (the Hydrological Modelling Framework for West Africa; Rameshwaran et al., 2021) and the Open Source (OS) LISFLOOD model (Van Der Knijff et al., 2010), thereafter referred to as LISFLOOD. ~~The HMF-WA model is adapted from the modular HMF model, and enhanced by Rameshwaran et al. (2021) to include additional key regional hydrological processes in the region such as wetlands, anthropogenic water use, and endorheic rivers (Rameshwaran et al., 2021). The HMF-WA simulates spatially~~

~~consistent river flows across West Africa at a 0.1° × 0.1° spatial resolution. Although the HMF-WA model has not yet been specifically calibrated to individual West African catchments using observed flow data where the model hydrology is configured to local conditions using spatial datasets of physical and soil properties, its evaluation against observational data indicates that it performs reasonably well in simulating both daily high and low river flows across most catchments. The median values of NSE (Nash-Sutcliffe efficiency), NSE_{log} and BIAS are 0.62, 0.82 and 0.06 (6 %), respectively (Rameshwaran et al., 2021). The LISFLOOD model is developed at the Joint Research Centre (JRC) of the European Commission (https://ec-jrc.github.io/lisflood/). LISFLOOD is a hybrid between a conceptual and fully physically based distributed rainfall-runoff model, designed for simulating the hydrological processes that occur in a catchment (Van Der Knijff et al., 2010). It supports a range of applications, including flood forecasting, water resources management, and climate change impact assessments. The LISFLOOD version used in this study (OS LISFLOOD v4.1.3) was calibrated using the discharge stations data described in the previous section, with a 0.05° (~5 km) resolution in its quasi-global implementation (-180, 180, 90, -60). This version of the LISFLOOD model, in combination with the 0.05° implementation maps (v1.1.1 openly available from https://global-flood.emergency.copernicus.eu/), has allowed the generation of the latest Copernicus Emergency Management Service Global Flood Awareness System (CEMS-GloFAS v4.0; https://www.globalfloods.eu/) reanalysis and forecast datasets.~~ The HMF-WA model is adapted from the modular HMF model, and is designed for large-scale applications across West Africa (Rameshwaran et al., 2021). It employs a vertically integrated soil moisture scheme to simulate runoff production, driven by rainfall and potential evaporation inputs. Runoff generation considers soil drainage and a spatial probability distribution of soil moisture. Routing is based on a kinematic wave approach (Bell et al., 2007), with parallel pathways for surface and subsurface flow. Key enhancements over the classical HMF model include modules to simulate wetland inundation, endorheic basins, and anthropogenic water withdrawals, making it well-suited for semi-arid environments with complex hydrology (Rameshwaran et al., 2021). HMF-WA simulates spatially consistent river flows across West Africa at a 0.1° × 0.1° spatial resolution. Although it has not yet been specifically calibrated to individual West African catchments using observed streamflow data where the model hydrology is configured to local conditions using spatial datasets of physical and soil properties, HMF-WA model evaluation against observational data indicates that it performs reasonably well in simulating both daily high and low river flows across most catchments. The

median values of NSE (Nash-Sutcliffe efficiency), NSElog, and BIAS are 0.62, 0.82, and 0.06 (6 %), respectively (Rameshwaran et al., 2021).

The LISFLOOD model, developed by the Joint Research Centre (JRC) of the European Commission (https://ec-jrc.github.io/lisflood/), is a physical, spatially distributed hydrological model, designed for simulating several hydrological processes that occur in a catchment (Van Der Knijff et al., 2010). The LISFLOOD model simulates water processes using a three-layer soil water balance, along with groundwater and subsurface flow models. It accounts for several processes such as snow accumulation/melt, infiltration, evapotranspiration, groundwater flow, surface runoff, etc. Moreover, it supports the integration of human influences such as reservoirs and water abstraction. The numerical LISFLOOD simulation is driven by meteorological forcing (precipitation, temperature, and evapotranspiration) combined with high-resolution spatial data on terrain morphology, soil characteristics, land use, and water demand. This integrated setup allows the model to simulate runoff processes under diverse climatic and socio-economic conditions, capturing both natural and anthropogenic influences across heterogeneous landscapes. The runoff produced at every grid cell within the model domain is routed through the river network using a kinematic wave approach. The LISFLOOD version used in this study (OS LISFLOOD v4.1.3) was calibrated with a 0.05° (~5 km) resolution in its quasi-global implementation covering a longitude range from -180° to 180° and a latitude range from 90° to -60°, using in-situ discharge gauge stations with at least four years of daily measurements recorded after 1 January 1982. In this setup, model parameters are linked to global geospatial datasets describing catchment morphology and river networks, land use, vegetation characteristics, soil properties, lake distribution, and water demand (Salamon et al., 2024; Choulga et al., 2024). The Distributed Evolutionary Algorithms in Python (DEAP; Fortin et al., 2012) framework was applied to optimize parameters in gauged catchments, with the modified Kling-Gupta Efficiency (KGE; Gupta et al., 2009) utilized as the objective function. Calibration was performed over a continuous simulation period using ERA5 reanalysis meteorological forcing. Due to the varying length and temporal coverage of the discharge records used for calibration, model performance was assessed using all available observational data at each station, rather than splitting the records into separate calibration and validation periods. The LISFLOOD calibration tool is freely available at https://github.com/ec-jrc/lisflood-calibration.

Globally, while both models use a kinematic wave routing scheme, HMF-WA and LISFLOOD differ significantly in their hydrological process representation. HMF-WA applies a vertically integrated soil moisture scheme with simplified runoff generation based on spatial soil moisture distribution. In contrast, LISFLOOD features a more detailed, physically-based three-layer soil model with an explicit representation of groundwater, snow processes, and anthropogenic influences. Furthermore, LISFLOOD has been calibrated using in-situ discharge data. Nevertheless, while calibration can enhance the accuracy of discharge simulations, several studies have highlighted that uncalibrated global hydrological models often exhibit comparable sensitivity to climate variability as the regional calibrated hydrological models, particularly when assessing relative changes in extreme events between future and historical periods (Gosling et al., 2017; Zhao et al., 2025). Therefore, whether a calibrated hydrological model offers different climate change projections than an uncalibrated model needs further investigation (Pechlivanidis et al., 2017).

2.4 Bias-corrected CMIP6 models and scenarios

The sixth phase of the Coupled Model Intercomparison Project (CMIP6) provides simulations from GCMs for the preindustrial period (1850–2014) and future climate projections (2015–2100) (Noël et al., 2022). To assess future climate impacts on floods, we have used five (5) daily GCMs rainfall and temperature outputs from the CMIP6 experiments (https://esgf-node.llnl.gov/search/cmip6). Table 1 gives the institute name and references of the CMIP6 climate models used in this study. These GCMS encompass a range of climate sensitivities, with Equilibrium Climate Sensitivity (ECS) values ranging from 2.98 to 5.34 (IPCC, 2021). The GCMs were selected based on their availability for the study area. Due to their accessibility, these GCMs have been widely used for climate impact assessments in Africa (Dosio et al., 2019; Almazroui et al., 2020; Klutse et al., 2021; Babaousmail et al., 2023; Nooni et al., 2023). The Cumulative Distribution Function-transform (CDF-t) (Michelangeli et al., 2009) was used to bias-correct the GCMs outputs. The CDF-t approach involves mapping the cumulative distribution function (CDF) from a GCM in the historical period to the observed CDF, then applying the same mapping to the GCM's future CDF (Flaounas et al., 2013; Pierce et al., 2015; Famien et al., 2018). The CDF-t method requires high-resolution observational data to work properly. The EWEMBI dataset (E2OBS, WFDEI, and ERA-I data, bias-corrected for ISIMIP; Frieler et al., 2017; Lange, 2018, 2019) was used to bias-correct the climate variables to drive the HMF-WA hydrological model. Similarly, the ERA5-land reanalysis

(Muñoz-Sabater et al., 2021). was used for bias-correcting the GCMs outputs for the LISFLOOD model. The EWEMBI dataset was developed to support bias correction of climate input data used in impact assessments in phase 2b of the Inter-Sectoral Impact Model Intercomparison Project (ISIMIP2b; Frieler et al., 2017). EWEMBI dataset (https://dataservices.gfz-potsdam.de/pik/showshort.php?id=escidoc:3928916) provides global spatial coverage with 0.5° x 0.5° spatial and daily temporal resolutions. It integrates multiple sources, including ERA-Interim reanalysis data (Dee et al., 2011), the WATCH Forcing Data methodology applied to ERA-Interim (WFDEI; Weedon et al., 2014), the eartH2Observe forcing dataset (E2OBS; Calton et al., 2016), and the NASA/GEWEX Surface Radiation Budget data (SRB; Stackhouse Jr. et al., 2011). Meanwhile, the ERA5 dataset is a global atmospheric reanalysis product developed by the Copernicus Climate Change Service (C3S) at ECMWF (European Centre for Medium-Range Weather Forecasts ReAnalysis). It is the fifth generation of atmospheric reanalysis based on 4D-Var (four-dimensional variational) data assimilation using Cycle 41r2 of the ECMWF Integrated Forecasting System (IFS) (Hersbach et al., 2020). ERA5 replaces the now outdated ERA-Interim reanalysis (Dee et al., 2011), and provides global spatial coverage from 1979 until the present, with a finer spatial and temporal resolution of 0.25° x 0.25° and 1 hour, respectively. The bias-corrected simulations are post-processed onto the 0.1° x 0.1° (~10 km x 10 km) HMF-WA model grid (Rameshwaran et al., 2021, 2022), and onto the 0.05° x 0.05° (~5 km x 5 km) LISFLOOD model grid for the period 1950-2100. CMIP6 models use five Shared Socioeconomic Pathways (SSPs). SSPs are an updated framework of climate scenarios, building upon the CMIP5 Representative Concentration Pathways (RCPs) while maintaining consistency in the 2100 radiative forcing levels. SSPs describe the socioeconomic factors (population growth, economic development, technological advancements, and governance) which can influence greenhouse gas emissions and adaptation strategies (O'Neill et al., 2017). Two Shared Socioeconomic Pathways (SSPs) are analysed in this study: the SSP2-4.5 (Middle of the Road) and the SSP5-8.5 (Fossil-Fueled Development). Rather than including the full range of SSPs, we focus on SSP2-4.5 and SSP5-8.5 narratives, which represent moderate and high emission trajectories, respectively. SSP2-4.5 is considered as a "middle-of-the-road" scenario, that is consistent with current national policies and moderate progress towards emission reduction commitments (). In contrast, SSP5-8.5 represents a high emissions pathway, allowing us to explore the upper limits of potential impacts under continued fossil fuel dependence and minimal climate policy intervention. While SSP5-8.5 has been criticized as an "overly pessimistic" narrative (Pielke & Ritchie, 2021), it

remains widely used in climate impact assessments to evaluate the vulnerability of socio-environmental systems under a "no-climate policy" world.

Table 1: Bias-corrected CMIP6 climate models used in this study

Institute	Climate Model	References
Max Planck Institute for Meteorology (Germany)	MPI-ESM1-2-HR	(Mauritsen et al., 2019)
Meteorological Research Institute (Japan)	MRI-ESM2-0	(Yukimoto et al., 2019)
Institute Pierre-Simon Laplace (France)	IPSL-CM6A-LR	(Boucher et al., 2020)
Met Office Hadley Centre (UK)	UKESM1-0-LL	(Mulcahy et al., 2020)
Geophysical Fluid Dynamics Laboratory (USA)	GFDL-ESM4	(Dunne et al., 2020)

2.5 Evaluation of hydrological models

The two hydrological models are evaluated over the period 1950-2014, which represents a compromise between the period covered by the ADHI database and the historical CMIP6 GCM simulations. To achieve this, we use the two-sample Anderson-Darling (AD) test at the 0.05 significance level (Scholz & Stephens, 1986) to compare the distributions of extreme values observed and simulated by the hydrological models. The null hypothesis of the AD test assumes that the simulated and observed AMF follow the same statistical distribution. The Block-Maxima approach (Gumbel, 1958) is used to construct extreme value time series, by extracting the annual maximum flow (AMF) from the daily discharge time series over the period 1950-2014. Unlike the Kolmogorov-Smirnov (KS) test (Berger & Zhou, 2014), which measures the maximum distance between two cumulative distribution functions (CDFs), the AD test assesses the overall distance between these CDFs, giving more weight to the tails of distributions. As a result, the AD test is more sensitive than the KS test in the tails of distributions and is therefore more suitable for comparing extreme values distributions (Engmann & Cousineau, 2011). That said, the AD test also has a limitation as the reliability of an empirical CDF can be affected by small sample sizes, particularly in the tails of the distribution. The performance of each hydrological model is given here by the proportion of CMIP6 simulations (among the 5) for which the AD test has failed. It is important to note that the AD test is only used herein to assess regional-scale performance of hydrological models, and not as a filtering criterion for inclusion or exclusion of models or stations.

2.6 Extremes Values Analysis Framework

2.6.1 The Generalized Extreme Value Distribution

According to the theory of extreme values, based on the Fisher–Tippett theorem, the Generalized Extreme Value (GEV) is the limiting distribution of independent and identically distributed random variables (Coles, 2001). The GEV is among the most frequently used distributions for extreme value analysis. It is a continuous three-parameter distribution that can account for non-stationarity, which refers to changes in statistical properties over time. This is achieved by allowing the parameters to vary as a function of time or other covariates (Hamdi et al., 2018; Wilcox et al., 2018). We, therefore, used the GEV to model the AMF series from each hydrological model simulations forced with the five CMIP6 climate models at each catchment. There are three parameters (location, scale and shape) in the GEV distribution (Hossain et al., 2021). In flood frequency analysis, each GEV parameter plays a distinct role in understanding and projecting flood behaviour~~, thus guiding effective flood risk management~~ (Lawrence, 2020; Wasko et al, 2021). The location parameter (μ) indicates the central tendency of flood magnitudes, with higher values suggesting a shift towards more frequent or severe floods. The scale parameter (σ) measures the variability or dispersion of the distribution, with larger values indicating greater uncertainty and a broader range of flood magnitudes. ~~The shape parameter (ξ) governs the tail behaviour of the distribution, with heavier tails suggesting an increased probability of extreme flooding events. This parameter is crucial for assessing the risk of rare floods and informing the design infrastructure to withstand such extremes.~~The shape parameter (ξ) governs the tail behaviour of the GEV distribution, which encompasses three types of extreme value distributions (Coles, 2001): (i) a positive shape parameter ($\xi > 0$) indicates a heavy-tailed Fréchet case (Fréchet, 1927), suggesting an increased probability of extreme flooding events, (ii) a null shape parameter ($\xi = 0$) suggests a light-tailed Gumbel class (Gumbel, 1958), and (iii) a negative shape parameter ($\xi < 0$) indicates a short-tailed or (bounded) negative-Weibull distribution (Weibull, 1951). This parameter is crucial for assessing the risk of rare floods and informing the design infrastructure to withstand such extremes. Equation (1) presents the cumulative distribution function (CDF) of the GEV (Coles, 2001).

$$F(x;u,\alpha,\xi) = exp\left\{-\left[1-\xi\frac{(x-u)}{\alpha}\right]^{1/\xi}\right\} \quad \kappa \neq 0 \tag{1}$$

$$F(x;\xi,\alpha) = exp\left\{-exp\left[-\frac{(x-u)}{\alpha}\right]\right\} \qquad \kappa = 0$$

Where x, u, α, et ξ are the data, location, scale, and shape parameters respectively, and $(u + \alpha/\xi) \leq x < \infty$ if $\xi < 0$; $-\infty < x < \infty$ if $\xi = 0$; $-\infty < x \leq (u + \alpha/\xi)$ if$\kappa > 0$.

Efficiently estimating the GEV parameters is crucial for the precise characterization and analysis of extreme events (Rai et al., 2024). ~~We have used the Generalized (Penalized) Maximum Likelihood Estimation (GMLE) method (Martins & Stedinger, 2000) to estimate the GEV parameters in a non-stationary context.~~We have used the Generalized (Penalized) Maximum Likelihood Estimation (GMLE) method (Martins & Stedinger, 2000) to estimate the GEV parameters in a non-stationary context, by allowing the model parameters to vary with time (Coles, 2001). The GMLE method overcomes the limitations of the well-known MLE (Fisher, 1992) method for small sample size (Hossain et al., 2021). To achieve this, Martins & Stedinger (2000) used a beta distribution (with shape parameters p = 6 and q = 9) as a prior to constraint the values of the GEV shape parameter in the interval [-0.5, +0.5], avoiding large negative values of the shape parameter. This approach has been used in several studies to estimate the GEV parameters in both stationary and non-stationary contexts (El Adlouni et al., 2007; Panthou et al., 2013; Tramblay et al., 2024). However, the original prior distribution from Martins & Stedinger (2000) is not well-suited for West Africa, as it results in shape parameter estimates below -0.5 for several stations, as illustrated in Supplementary Figure S3~~2~~. Here, we therefore use a normal distribution as a prior for the GMLE method. This normal distribution is fitted to the GEV shape parameter values estimated on 98 AMF series spanning a minimum of 20 years over the period 1950-2018 from the ADHI database Tramblay et al. (2021) using the L-moments method (Hosking, 1990). ~~The newly developed regional prior, modelled as a normal distribution, has a mean of -0.24 and a standard deviation of 0.16 (see Supplementary Figure S2).~~The newly developed regional prior, modelled as a normal distribution, has a mean of -0.24 and a standard deviation of 0.16 (see Supplementary Figure S3), and is used to fit the GEV distribution to the historical and projected annual peak flood time series generated by hydrological models driven by the CMIP6 GCMs.

2.6.2 Determining magnitude and direction of changes in flood events

To analyse future changes in floods, we compare two 30-year future periods (a near-term future [2031–2060] and a long-term future [2071–2100]) to a reference historical period (1985-2014) at stations where there is a good fit between observed (OBS) AMF series and hydrological models simulations (HIST) according to the Anderson-Darling (AD) test (at 0.05 level), and also in stations at which the null hypothesis of the AD test is rejected. We have chosen to work with the 2-year and 20-year floods to analyse the impacts of climate change in West Africa. The 2-year return period indicates relatively frequent flood events, and this information is essential for understanding and managing risks associated with flooding. The 20-year flood event is frequently used for comparative purposes in various studies, as it balances the rarity of extreme events (data length limitations) and the uncertainty in the estimated return levels (Dawson et al., 2005; Tramblay & Somot, 2018; Han et al., 2022). Thus, the 2- and 20-year flood quantiles are computed at each station for the three 30-year periods using the GEV model fitted to the AMF series by the GMLE method. Changes in flood are quantified in this study by computing the ratio of the difference between the future flood quantile (Qfuture) and the historical flood quantile (Qhist) to Qhist itself. To assess the statistical significance of the differences between the historical and future flood quantiles, we have used the parametric bootstrapping approach. After estimating the GEV distribution parameters, we have generated 2500 simulations of annual peak floods for each subperiod (with each simulation representing a sample of 30 data points). We have then recomputed the 2-year and 20-year flood quantiles for each simulation. The significance of the differences between the quantiles was evaluated at the 0.05 level. It is crucial to consider the degree of consensus among multiple climate models to reduce the potential noise in the projections and reach robust conclusions (Awotwi et al., 2021; Dosio et al., 2021)**.** Here we have computed a multi-model index of agreement (MIA) as introduced by Tramblay & Somot (2018), to present the results in terms of the proportion of CMIP6 models projecting significant change for each station. The MIA allows the assessment of the robustness of climate model projections, ensuring cross-catchment comparability due to its standardised scale ranging from -1 to 1, according to the direction of change (i.e., MIA = 1 (-1) if all models project an increasing (decreasing) trend).

$$MIA = \frac{1}{n}\left(\sum_{i=m}^{n} i_m\right) \quad (2)$$

From equation (6), for a given CMIP6 model (m), $i_m = 1$ for regionally significant upward trends, $i_m = -1$ for significant negative trends, and $i_m = 0$ when no significant trends are detected, across n climate simulations.

2.6.3 Determining temporal functions for GEV parameters and modelling of non-stationary extreme values

While the previous section focused on the magnitude and direction of changes in flood events under different scenarios, this section describes the methodology used to identify when these changes began. Understanding how the parameters of the GEV distribution might shift under future climate scenarios is a critical question that needs to be addressed given the accelerating impacts of global warming on environmental conditions. Answering this question can inform a more reliable modelling process to estimate flood quantiles. Several studies have suggested that both the location and scale parameters of the GEV distribution should be adjusted proportionally to account for the effects of climate change (Stedinger & Griffis, 2011; Prosdocimi & Kjeldsen, 2021; Jayaweera et al., 2024). Here, to determine the appropriate temporal function for the non-stationary GEV, the trends in GEV parameters are detected using the non-parametric Mann-Kendall test (Mann, 1945; Kendall, 1975). As the test is applied to parameters estimated over moving windows, it is important to note that temporal correlation is introduced, which can bias the results of the original Mann-Kendall test, as it assumes independence of observations. To address this, we have applied a modified version of the test based on the Hamed & Rao (1998) variance correction approach, specifically adapted for serially correlated data. A window size of 30 years has been selected to ensure sufficient data to fit the ~~SGEV~~stationary GEV model (SGEV), with a total of 121 windows. For each window, each hydrological model (LISFLOOD and HMF-WA) and each climate scenario (SSP2-4.5 and SSP5.8-5), the SGEV is fitted to AMF series from the averaged hydrological simulations driven by data from the CMIP6 models. The Mann-Kendall test is then applied to the series of estimated parameters at the 0.05 significance level.

Based on the results of the trend analysis of the GEV parameters, the location (μ) and scale (σ) parameters are expressed as linear functions of time, denoted as $\mu(t)$ and $\sigma(t)$, while the shape parameter remains constant. Thus, the non-stationary GEV model involves a vector $\psi=[\mu 0;\mu 1;\sigma 0:\sigma 1:\xi]$ of five unknown parameters. We have decided to keep the shape parameters constant because it is uncommon for researchers to model all three GEV parameters as covariate-dependent functions. Indeed, adding this level of complexity can significantly complicate the model parameters estimation, particularly the shape parameter (Katz, 2013;

Papalexiou & Koutsoyiannis, 2013). Allowing any starting date (year t_0) of a possible significant trend in the GEV location and scale parameter, we have considered three cases of the non-stationary GEV (NSGEV; cf. Equations 3-5):

- Case 1 (GEV1): a linear trend with no breakpoint (i.e., a single trend over the entire record for both the location and scale parameters):

$$\mu(t) = \mu_0 + \mu_1 t \; ; \; \sigma(t) = \sigma_0 + \sigma_1 t \qquad \text{for} \quad t \leq t_0 \tag{3}$$

- Case 2 (GEV2): a linear trend after a breakpoint (i.e., the location and scale parameters are constant before the year t_0 and linearly dependent on time after t_0):

$$\begin{aligned} &\mu(t) = \mu_0 \; ; \; \sigma(t) = \sigma_0 && \text{for} \quad t \leq t_0 \\ &\mu(t) = \mu_0 + \mu_1(t-t_0) \; ; \; \sigma(t) = \sigma_0 + \sigma_1(t-t_0) && \text{for} \quad t \geq t_0 \end{aligned} \tag{4}$$

- Case 3 (GEV3): both trends before and after a breakpoint are considered (i.e., a linear trend before and after year t_0 for both location and scale parameters):

$$\begin{aligned} &\mu(t) = \mu_0 + \mu_1(t_0-t) \; ; \; \sigma(t) = \sigma_0 + \sigma_1(t_0-t) && \text{for} \quad t \leq t_0 \\ &\mu(t) = \mu_0 + \mu_1(t-t_0) \; ; \; \sigma(t) = \sigma_0 + \sigma_1(t-t_0) && \text{for} \quad t \geq t_0 \end{aligned} \tag{5}$$

Unlike in Wilcox et al. (2018), where breakpoints are defined independently for $\mu(t)$ and $\sigma(t)$, in the present study, we assume a common breakpoint for both parameters. This means that both $\mu(t)$ and $\sigma(t)$ change simultaneously at the same point in time. To ensure that the NSGEV model is fitted with sufficient data, the first start year is set no earlier than 20 years after the beginning of the time series (1950) and the last start year is set no later than 20 years before the end of the time series (2100). Thus, the possible starting years of change (t_0) fall between 1970 and 2070. There are as many NSGEV models as there are breakpoints or starting years, and the non-stationary model with the highest log-likelihood is selected (see Supplementary Figure S~~3~~4). The procedure described above is inspired by several studies that focused on detecting trends in hydroclimatic time series using non-stationary GEV (Hawkins & Sutton, 2012; Panthou et al., 2013; Blanchet et al., 2018; Hamdi et al., 2018; Tramblay & Somot, 2018; Wilcox et al., 2018).

Once the best breakpoint has been determined for each time-varying GEV model based on the log-likelihood profile, the trend models (GEV1, GEV2 and GEV3) are compared with each

other using the Akaike information criterion (AIC; Akaike, 1974). The AIC criterion is widely used to compare multiple statistical models by assessing their goodness-of-fit. It accounts for the trade-off between a model's fit to the data and its complexity, by penalising for more complex models. While a more complex model may provide a better fit, it often does not provide sufficient improvement to justify the addition of extra parameters (Wilcox et al., 2018). Thus, the AIC is well-suited for evaluating the performance of non-stationary GEV models. Furthermore, a deviance test (D) based on likelihood ratio (LR; Coles, 2001) is performed at the 0.05 significance level between the best GEV trend model selected previously based on the AIC criterion and the stationary GEV model (SGEV). The LR test allows us to determine the best model between two competing nested models by comparing the D-statistic given by Equation (6) to the chi-square (x^2) distribution.

$$D = 2\{\log(ML_{NSGEV}) - \log(ML_{SGEV})\} \quad (6)$$

From Equation (6), D represents the deviance test statistic value (referred to as D-statistic above), $\log(ML_{NSGEV})$ and $\log(ML_{SGEV})$ are the maximised log-likelihood functions of the NSGEV and the SGEV, respectively. Letting c_α be the (1 - α) quantile of the chi-square distribution (where α represents the level of significance), with υ degrees of freedom equal to the difference in the number of model parameters between the non-stationary and stationary models, the non-stationary GEV is accepted at the level α if the D-statistic is greater than c_α, meaning a significant trend in the data.

~~To reduce Type 1 errors (Mudge et al., 2012) that could arise from the deviance test based on the likelihood ratio and assess the field significance of the detected local trends, the False Discovery Rate (FDR) procedure is implemented (Hochberg & Benjamini, 1995). The FDR procedure aims to reduce the proportion of false positives among the null hypothesis local rejections by adjusting the vector of p-values from the set of at-site tests (Wilks, 2006). The FDR approach has been used in many studies of hydroclimatic variables due to its advantages over other methods, such as dealing with spatial autocorrelation (Khaliq et al., 2009). For consistency with local deviance and MK tests, the FDR procedure is computed at 0.05 global significance level (α_{global}). The FDR test rejects the local null hypothesis when the corresponding p-value is lower than α_{global}. If the null hypothesis is rejected at least once within the study area, field significance is then declared (Wilks, 2016).~~The null hypothesis of the deviance test assumes that the stationary GEV model provides a better fit to the data than the non-stationary model, indicating that there is no significant trend in the AMF. However, the

presence of spatial cross-correlations across stations may bias the results of simultaneous multiple local tests by increasing the likelihood of detecting false positives (Farris et al., 2021). To assess the field significance of local trends detected in AMF series in the study area, we implement the False Discovery Rate (FDR) procedure (Hochberg & Benjamini, 1995). The FDR's null hypothesis assumes that none of the stations across the region exhibits a significant trend in AMF (i.e., all local null hypotheses are actually true). The FDR aims to reduce Type 1 errors (Mudge et al., 2012), by adjusting the vector of p-values from the set of at-site tests (Wilks, 2006). Due to its advantages over other methods, such as dealing with spatial autocorrelation, the FDR approach has been used in many studies of hydroclimatic variables (Khaliq et al., 2009). For consistency with local deviance and MK tests, the FDR procedure is computed at 0.05 global significance level (αglobal). The FDR test rejects the local null hypothesis when the corresponding FDR-adjusted p-value is lower than αglobal. Field significance is declared if the local null hypothesis is rejected at least once within the study area (Wilks, 2016).

3 Results and discussions

3.1 Assessing the performance of hydrological models

The two hydrological models' performance is assessed over the period 1950-2014 by applying the two-sample Anderson-Darling (AD). The results of the statistical evaluation of the two hydrological models are shown in Figure 2. The performance of each model at each station is assessed based on the proportion of CMIP6 models that fail the Anderson-Darling test at the 0.05 significance level. Specifically, if more than two out of five CMIP6 simulations fail the test at a given station, the hydrological model is considered to perform poorly at that station. Considering this evaluation criterion, the LISFLOOD hydrological model performs well at 64 % of the stations, while the HMF-WA model performs satisfactorily at only 24 % of the stations (Figure 2). ~~Although both models are semi-physically based and spatially distributed, the LISFLOOD model outperforms the HMF-WA model in simulating extreme flows in West Africa (Figure 2). This difference in performance can be attributed to several factors: (i) the LISFLOOD model was run at a finer resolution (0.05° x 0.05°) compared to the coarser resolution of 0.1° x 0.1° used by the HMF-WA model (Rameshwaran et al., 2021); (ii) the HMF-WA model includes fewer meteorological forcings and only a limited number of~~

~~hydrological processes (specifically wetlands, anthropogenic water use, and endorheic rivers), whereas the LISFLOOD model can incorporate over 70 different processes depending on the target application (i.e., rainfall-runoff transformation, flood and drought forecasting) and the required level of configuration (more detailed information on the configuration of LISFLOOD can be found at https://ec-jrc.github.io/lisflood-model; and (iii) the HMF-WA model has not been calibrated to individual west African catchment conditions with observed flow data (Rameshwaran et al., 2021). In contrast, the LISFLOOD model, in its quasi-global implementation, has been calibrated using in-situ discharge observations covering several river basins worldwide, including most West African basins, and with discharge time series spanning at least four years after 01 January 1980. Consequently, while the distributed nature of the HMF-WA model aims to improve the understanding of regional climate change impacts in a spatially coherent manner across West Africa, it does not necessarily lead to better modelling of extreme flows in the various climates and socioeconomic contexts of the region without calibration.~~ Although both models are semi-physically based and spatially distributed, the LISFLOOD model outperforms the HMF-WA model in simulating extreme flows in West Africa (Figure 2). These findings are consistent with those of Ekolu et al. (2025), who reported that the LISFLOOD model effectively simulates the hydrological cycle and captures the specific characteristics of hydrological droughts and floods in West Africa. This difference in performance can be attributed to several factors: (i) the LISFLOOD model was run at a finer resolution (0.05° x 0.05°) compared to the coarser resolution of 0.1° x 0.1° used by the HMF-WA model (Rameshwaran et al., 2021); (ii) the HMF-WA model includes fewer meteorological forcings and only a limited number of hydrological processes (specifically wetlands, anthropogenic water use, and endorheic rivers), whereas the LISFLOOD model can incorporate over 70 different processes depending on the target application (i.e., rainfall-runoff transformation, flood and drought forecasting) and the required level of configuration (more detailed information on the configuration of LISFLOOD can be found at https://ec-jrc.github.io/lisflood-model; and (iii) the HMF-WA model has not been calibrated to individual west African catchment conditions with observed flow data, and its performance depends on the accuracy of spatial datasets of physical and soil properties (e.g., wetlands, anthropogenic water use, and endorheic rivers) used to configure the model's hydrology to local conditions (Rameshwaran et al., 2021). In contrast, the LISFLOOD model has been regionally calibrated using in-situ discharge observations, with discharge time series spanning at least four years after 01 January 1982. Consequently, while the distributed nature of the HMF-WA model aims to improve the understanding of regional climate change impacts in a spatially coherent manner

across West Africa, it does not necessarily lead to better modelling of extreme flows in the various climates and socioeconomic contexts of the region without calibration. Runoff generation is inherently a spatially distributed process. As such, the spatial resolution of a distributed hydrological model can significantly affect its ability to capture spatial variability of key watershed characteristics, such as topographic features, land cover heterogeneity, and precipitation gradients (Wolock & Price, 1994; Haddeland et al., 2002). A coarser spatial resolution limits the level of detail that can be represented in hydrological simulations, potentially overlooking important small-scale processes. Furthermore, as hydrological models are simplified representations of complex watershed processes, a calibration phase is often necessary to compensate for limited information on spatial variability of physiographical and meteorological catchments attributes, and to improve model performance in simulating the watershed's hydrological cycle (Bruneau et al., 1995). However, many river basins in West Africa have a limited number of in situ observational networks to provide the current state of hydrological information (Ndehedehe, 2019). This limits the optimal parameterization of large-scale hydrological models and may introduce uncertainties in model outputs. In addition, the satisfactory performance of the LISFLOOD model indicates that, although a flood-centered calibration approach could potentially improve its ability to capture extreme flows and their trends (Wasko et al., 2021), the current model setup provides a satisfactory basis for regional-scale flood trend assessments.

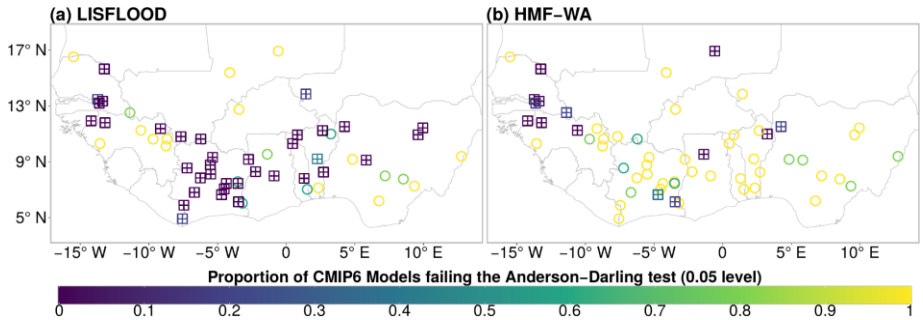

~~Figure 2: Statistical evaluation of the two hydrological models: a) Two-sample Anderson-Darling (AD) goodness-of-fit (GOF) test at 0.05 statistical significance level at each station between the AMF of daily OBS from the ADHI database and annual maxima flow of HIST from LISFLOOD daily simulations forced with the five CMIP6 GCMs (GFDL, IPSL, MPI, MRI, and UKESM) over the period 1950-2014. b) same as a) but using HMF-WA as hydrological model. The Performance of each hydrological model is given by the proportion of CMIP6 simulations for which the AD test has failed. The circles show stations where 60-~~

~~100 % of CMIP6 models fail the test, and squares represent stations where 0–20 % of CMIP6 models fail the AD test.~~

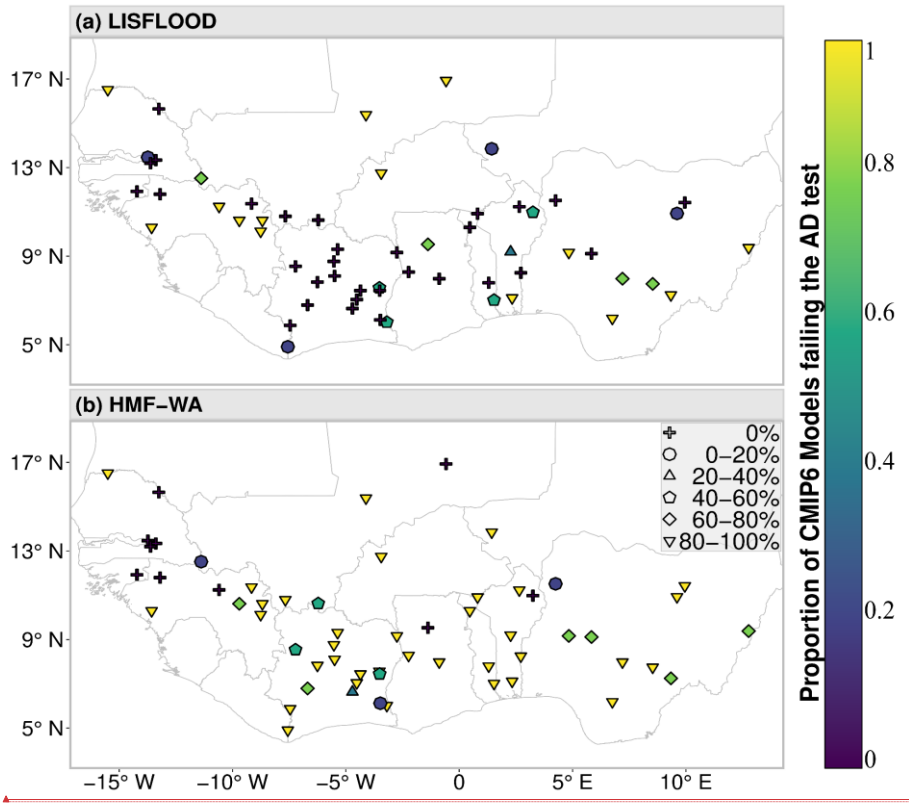

Figure 2: Statistical evaluation of the two hydrological models: a) Two-sample Anderson-Darling (AD) goodness-of-fit (GOF) test at 0.05 statistical significance level at each station between the AMF of daily OBS from the ADHI database and annual maxima flow of HIST from LISFLOOD daily simulations forced with the five CMIP6 GCMs (GFDL, IPSL, MPI, MRI, and UKESM) over the period 1950-2014. b) same as a) but using HMF-WA as hydrological model. The fill color of the markers indicates the proportion of CMIP6 models (out of five) for which the AD test null hypothesis (i.e., simulated and observed AMF follow the same statistical distribution) is rejected at the 0.05 significance level. Marker shapes correspond to binned categories of this proportion, as indicated in the legend.

To further assess the performance of the hydrological models in capturing extreme flows, we computed the Relative Bias between the AMF simulated by the LISFLOOD-CMIP6 and HMF-WA-CMIP6 hydrological models and the observed AMF from the ADHI database. This

a mis en forme : Police :11 pt

a mis en forme : Police :11 pt

a mis en forme : Espace Après : 0 pt, Interligne : Multiple 1,15 li

a mis en forme : Police :11 pt

comparison was performed over the historical period (1950–2014), focusing on the climatological characteristics of AMF (median values) rather than on year-to-year correspondence. This approach allows us to evaluate whether the hydrological models tend to overestimate or underestimate flood peaks, considering climate models individually. As shown in Figure 3, the HMF-WA model consistently shows a negative relative bias across all GCMs, with median values ranging from -52 % (IPSL) to -46 % (UKESM) across the region. These negative biases suggest a tendency of the HMF-WA model to underestimate peak flow. The LISFLOOD model, in contrast, shows lower bias than the HMF-WA model, with a mix of slight underestimations and even overestimations (Figure 3). For instance, the median values for the LISFLOOD model simulations range from -14 % (MPI) to 7 % (GFDL). Although the LISFLOOD model also shows negative biases with most GCMs, such as IPSL, MPI, MRI, and UKESM, the magnitude of these biases is much smaller compared to the HMF-WA model. Nevertheless, whether a calibrated hydrological model offers more reliable climate change projections than an uncalibrated model, which may perform less accurately in reproducing historical conditions (Pechlivanidis et al., 2017), remains questionable. Examining whether their capacity to simulate hydrological responses to historical climate is influencing projected trends for climate change impacts remain important, especially considering that most projections of climate change impacts on African hydrological trends were produced using uncalibrated models (Davie et al., 2013; Sauer et al., 2021).

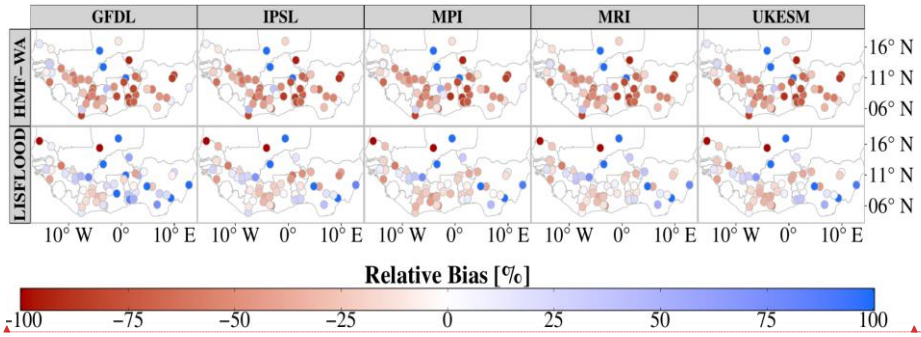

Figure 3: Relative bias (percentages) computed between simulated AMF from LISFLOOD-CMIP6 and HMFWA-CMIP6 hydrological models' simulations, and observed AMF from the ADHI database, for the historical period (1950-2014).

3.2 Magnitude and direction of changes in flood events

a mis en forme : Police :11 pt
a mis en forme : Police :11 pt
a mis en forme : Police :11 pt
a mis en forme : Police :11 pt
a mis en forme : Police :11 pt, Non Gras
a mis en forme : Police :11 pt, Non Gras

To analyse changes in floods, we have compared two 30-year future periods (a near-term future [2031–2060] and a long-term future [2071–2100]) to a reference historical period (1985-2014). To achieve this, we have fitted the GEV distribution the AMF series of each model simulation using the GMLE method. Then, the 2- and 20-year flood quantiles are computed at each station for the three 30-year periods. Figure 4 shows the MIA on the direction of changes in the 2-year and 20-year floods for the near-term and long-term futures, from both LISFLOOD and HMF-WA models simulations under SSP2.4-5 and SSP5.8-5 scenarios. Despite their differences in terms of hydrological processes representation (model structures) and input data, the two hydrological models generally projected consistent impacts of climate change on future floods across the West African region. Both hydrological models consistently project an increase (positive change) in floods in the near-term and long-term futures across West Africa (Figure 4).

a mis en forme : Police :11 pt

a mis en forme : Police :11 pt

In the near-term future (2031–2060), there is a high level of agreement in projecting positive changes in the 2-year flood event under both SSP2-4.5 and SSP5-8.5 scenarios. The simulations of the LISFLOOD and HMF-WA models show strong agreement across the CMIP6 models. Under SSP2-4.5, the MIA values range from -0.2 to 1 for the LISFLOOD model (Figure 4a-1), and from -0.2 to 0.8 for the HMF-WA model (Figure 4b-1). This agreement increases for both hydrological models under SSP5-8.5, with MIA values falling between -0.2 and 1 for both LISFLOOD (Figure 4a-3) and HMF-WA models (Figure 4b-3). The consistent climate change impact projections suggest that more frequent flood events are expected to become increasingly common across the West African region. For the 20-year flood event, which is less frequent but more severe, MIA values range from -0.2 to 0.8 (-0.2 to 1) and from 0 to 0.8 (0 to 1) under the SSP2-4.5 (SSP5-8.5) for the LISFLOOD (Figure 4a-2 and Figure 4a-4) and HMF-WA (Figure 4b-2 and Figure 4b-4) models, respectively.

a mis en forme : Police :11 pt

In the long-term future (2071–2100), considering the 2-year flood, MIA values range from -0.6 to 1 (-0.6 to 0.8) and from -0.6 to 0.6 (0.4 to 0.8) under the SSP2-4.5 (SSP5-8.5) for the LISFLOOD (Figure 4a-5 and Figure 4a-7) and HMF-WA (Figure 4b-5 and Figure 4b-7) models, respectively. For the 20-year flood, model agreement in projecting the positive changes in flood magnitude remains relatively high, with MIA values ranging from -0.4 to 0.6 (-0.4 to 0.8) and from 0 to 0.6 (-0.2 to 0.8) under the SSP2-4.5 (SSP5-8.5) for the LISFLOOD (Figure 4a-6 and Figure 4a-8) and HMF-WA (Figure 4b-6 and Figure 4b-8) models, respectively. It is also worth noting that negative changes are projected in the 2-year flood in the long-term future

in a few sets of catchments located in the western part of the region (Figure 4a-5, 4a-7, 4b-5 and 4b-7). This area is also projected to experience a decrease in annual rainfall when looking at the full CMIP6 ensemble (IPCC, 2021). However, the agreement between the CMIP6 models remains very weak, indicating a lower confidence in the robustness of these negative changes compared to the regional pattern. Overall, the agreement between the CMIP6 and the hydrological models is higher for the near-future than for the long-term future, reflecting increased uncertainty as the projection timeline extends.

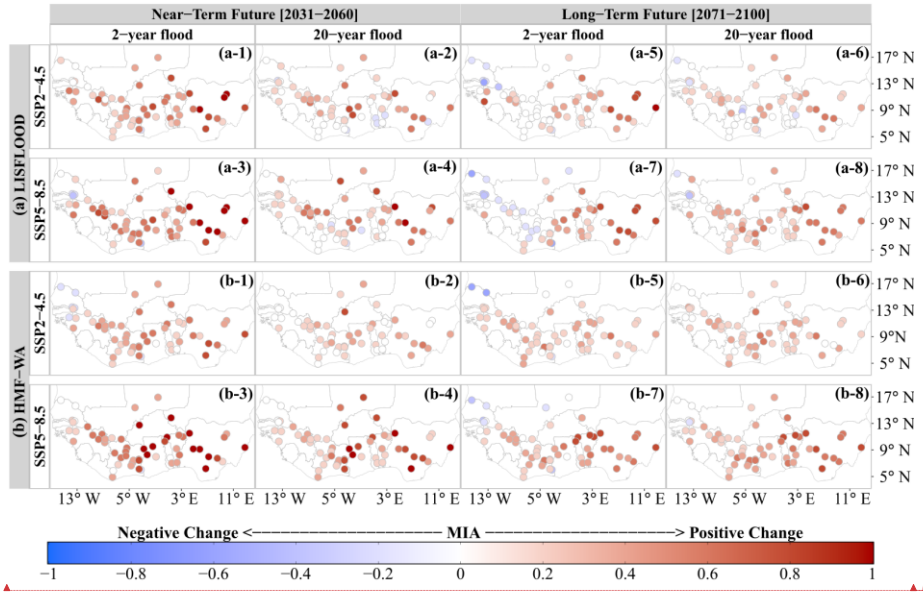

Figure 4: Spatial distribution of the multi-model index of agreement (MIA) on the direction of changes in 2-year and 20-year flood events for the near-term (2031-2060) and long-term (2071-2100) futures, compared to the historical reference period (1985-2014). This analysis combines simulations from: (a) LISFLOOD and (b) HMF-WA hydrological models, forced with five bias-corrected CMIP6 models (GFDL, IPSL, MPI, MRI, and UKESM), under the SSP2.4-5 (a1 to a4 and b1 to b4) and SSP5.8-5 (a5 to a8 and b5 to b8) scenarios. Flood quantiles are estimated using the GEV distribution fitted with the GMLE method. Negative change (decrease in flood quantiles) is represented by shades of blue, and positive change (increase in flood quantiles) is represented by shades of red.

Figure 5 summarises the projected climate impacts on floods in the near-term (2031-2060) and long-term (2071-2100) futures in West Africa across the different CMIP6 models (GFDL, IPSL, MPI, MRI, and UKESM). Both hydrological models' simulations consistently suggest

a mis en forme : Police :11 pt
a mis en forme : Police :11 pt
a mis en forme : Police :11 pt
a mis en forme : Police :11 pt
a mis en forme : Police :11 pt

strong changes in floods, with most median values falling above the zero-change baseline. Considering the CMIP6 models' projections individually in the near-future, under both SSP2-4.5 (Figure 5a) and SSP5-8.5 (Figure 5b) scenarios, the most pronounced changes are obtained for both hydrological models when forced with IPSL, MRI, and UKESM models. These near-term projections highlight the potential for more frequent extreme flood events, leading to increased flood risks and greater socioeconomic vulnerability in the West African region. In the long-term future, the distribution of flood trends is quite consistent between the two hydrological models, and the variability stems only from GCMs. For instance, under SSP2-4.5, the variability between the different CMIP6 models is very pronounced, with most projections showing relatively modest changes compared to the SSP5-8.5 scenario, where most of the GCM agree for a positive change in floods magnitudes.

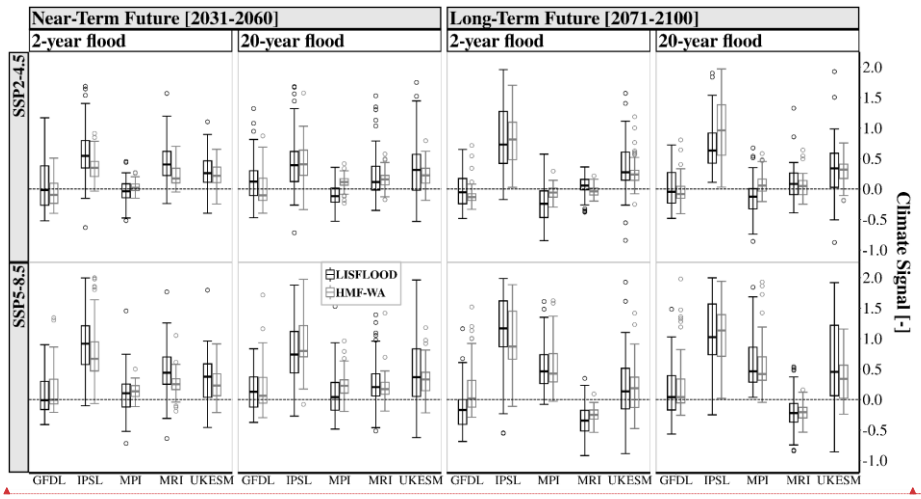

Figure 5: Synthesis of the projected changes in the 2-year and 20-year floods in West Africa from the LISFLOOD (black boxplots) and HMF-WA (grey boxplots) model simulations forced with the five CMIP6 GCMs (GFDL, IPSL, MPI, MRI, and UKESM), under both SSP2-4.5 (top row) and SSP5-8.5 (bottom row) climate scenarios, for the near-term (2031-2060) and the long-term (2071-2100) futures. The climate signal (y-axis) refers to the relative change in flood magnitude, computed as the difference between the future flood quantile (Qfuture) and the historical flood quantile (Qhist), normalized by Qhist. The black dotted line represents the zero-change baseline.

~~To further assess the agreement between the two hydrological models, Figure 6 shows the scatter plots illustrating how projected changes (Δ Flood) in floods compares between~~

a mis en forme : Police :11 pt
a mis en forme : Police :11 pt
a mis en forme : Police :11 pt
a mis en forme : Police :11 pt
a mis en forme : Police :11 pt

~~LISFLOOD and HMF-WA model simulations. Overall, both models project positive change in floods in West Africa regardless of the climate scenario considered. Indeed, most data points fall above the zero-change baseline, indicating a global positive change in floods from both hydrological model simulations (Figure 6). To confirm the agreement between the two models, we have computed the Spearman coefficient (ρ) between the projected multi-model mean changes in floods (Δ Flood) from the simulations of the LISFLOOD and HMF-WA models.~~To further assess the agreement between the two hydrological models, Figure 7 displays how the projected multi model mean changes in floods (ΔFlood) compares between LISFLOOD and HMF-WA model simulations. Overall, both models project positive change in floods in West Africa regardless of the considered SSP scenario. Indeed, most data points fall above the zero-change baseline, indicating a global positive change in floods from both hydrological model simulations (Figure 7). To confirm the agreement between the two models, we have computed the Spearman coefficient (ρ) between the ΔFlood from the simulations of the LISFLOOD and HMF-WA models. ~~Supplementary Table S1 gives the Spearman coefficient (ρ) values for the 2-year and the 20-year floods, under the SSP2-4.5 and SSP5-8.5 scenarios.~~ The correlation analysis shows that the agreement between the two models is particularly pronounced~~.~~ under the SSP5-8.5 scenario, suggesting a stronger influence of climatic changes under the high emissions scenario. In the near-term future, the Spearman correlation coefficient is 0.75 (0.64) for the 2-year (20-year) floods. In the long-term future, the correlation remains high, with 0.72 (0.70) for the 2-year (20-year) floods, suggesting that the models continue to show strong agreement, even for long-term projections. These results indicate a relatively high level of consistency between the two hydrological models for projecting future flood changes, despite the systematic biases in HMF-WA model over the reference historical period. Thus, using both models, the climate forcing has more importance than the hydrological representation itself.

a mis en forme : Police :11 pt

a mis en forme : Police :11 pt

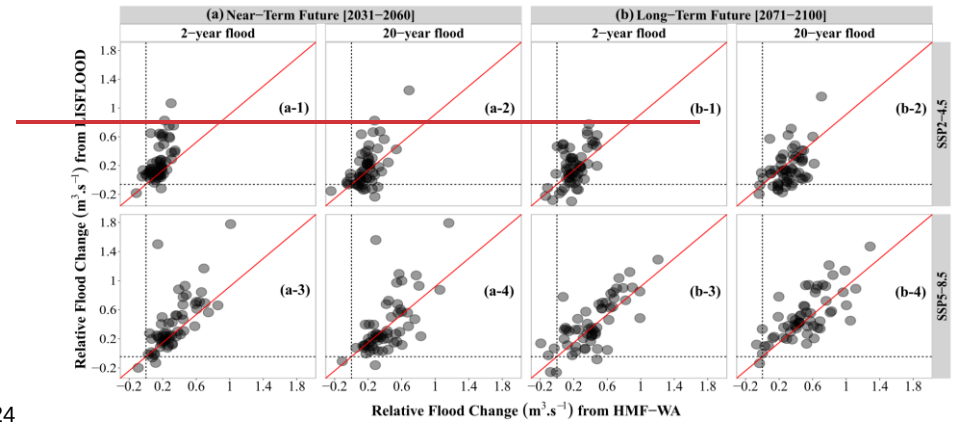

~~Figure 6: Comparison of projected multi-model mean changes in flood (Δ Flood) between LISFLOOD and HMF-WA hydrological models, under SSP2.4-5 and SSP5.8-5 scenarios, for the near-term (2031-2060) and the long-term futures (2071-2100), compared to the historical reference period (1985-2014). The gray dashed lines represent the zero-change baseline and the red diagonal line represents the theoretical 1:1 line where projected changes from both hydrological models would be identical.~~

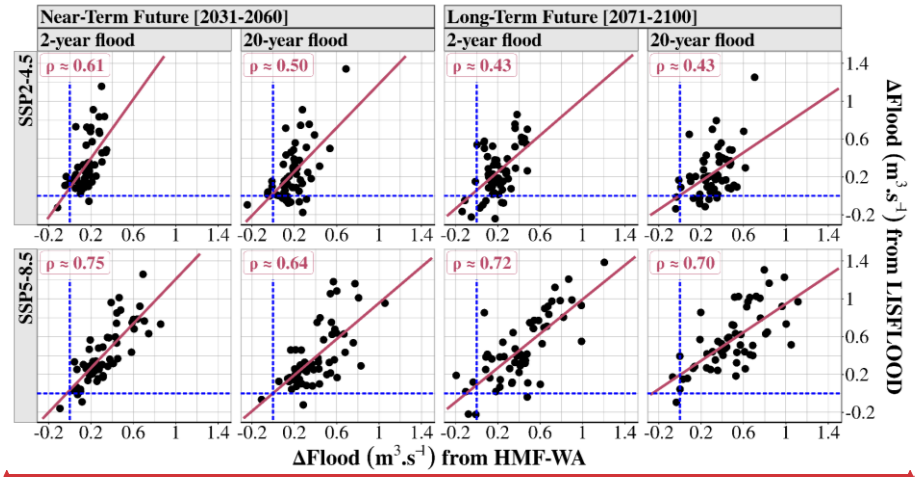

Figure 6: Comparison of projected multi model mean changes in flood (ΔFlood) between LISFLOOD and HMF-WA hydrological models, under SSP2.4-5 (top row) and SSP5.8-5 (bottom row) scenarios, for the near-term (2031-2060) and the long-term futures (2071-2100), compared to the historical reference period (1985-2014). The blue dashed lines represent the zero-change baseline and the red diagonal line represents the theoretical 1:1 line where projected changes from both hydrological models would be identical.

a mis en forme : Police :11 pt

a mis en forme : Police :11 pt, Gras

a mis en forme : Police :11 pt, Gras

a mis en forme : Espace Avant : 0 pt, Interligne : Multiple 1,15 li

838 The relative magnitude of change in floods was also analysed by computing the mean relative
839 change. (i.e., ratio of the difference between the flood quantiles of the future periods and the
840 reference historical period) across CMIP6 models for each hydrological model. The spatial
841 distribution of the magnitude of changes, as simulated with the LISFLOOD and HMF-WA
842 hydrological models under both SSP2-4.5 and SSP5-8.5, is shown in Figure 7a and Figure 7b,
843 respectively. Supplementary Table S~~3~~2 summarises the overall mean relative change in floods
844 across the region from both hydrological model's simulations. The two hydrological models
845 consistently project an increase in future floods across the West African region, with flood
846 magnitudes at most sites exceeding 50 %, particularly under SSP5-8.5 (Figure 7a-3, 7a-4, 7a-
847 7, 7a-8, 7b-3, 7b-4, 7b-7, and 7b-8). These results are consistent with previous studies that
848 argued for the ongoing rising trend in extreme streamflow across the West African catchments
849 (Nka et al., 2015; Aich et al., 2016; Wilcox et al., 2018; Ekolu et al., 2025). However, a
850 common limitation of most previous studies is their reliance on a relatively small sample of
851 watersheds and a limited spatial coverage, which may overlook local hydrographic variability
852 and limit regional applications. In addition, most impact studies in West Africa are based on
853 conceptual hydrological models at catchment scales. The study differs from previous studies
854 by covering an unprecedented set of catchments, and utilizing state-of-the-art bias-corrected
855 CMIP6 climate models, two large-scale hydrological models and robust statistical methods to
856 assess both the magnitude and field significance of future flood changes. As such, the findings
857 from this work provide regional-scale insights into the evolving flood risks in West Africa.
858 Furthermore, the findings from the studies of Almazroui et al. (2020), Dosio et al. (2021) and
859 Dotse et al. (2023) have shown that CMIP6 models contain a robust signal of the intensification
860 of the rainfall regime in West Africa. The increasing trend in floods across the region may be
861 partly explained by the trends in extreme precipitations, as their variability influences the
862 hydrological dynamics of the region (Panthou et al., 2013; Wilcox et al., 2018; Elagib et al.,
863 2021).

a mis en forme : Police :11 pt, Gras

a mis en forme : Police :11 pt, Gras

a mis en forme : Police :11 pt, Gras

a mis en forme : Police :11 pt, Gras

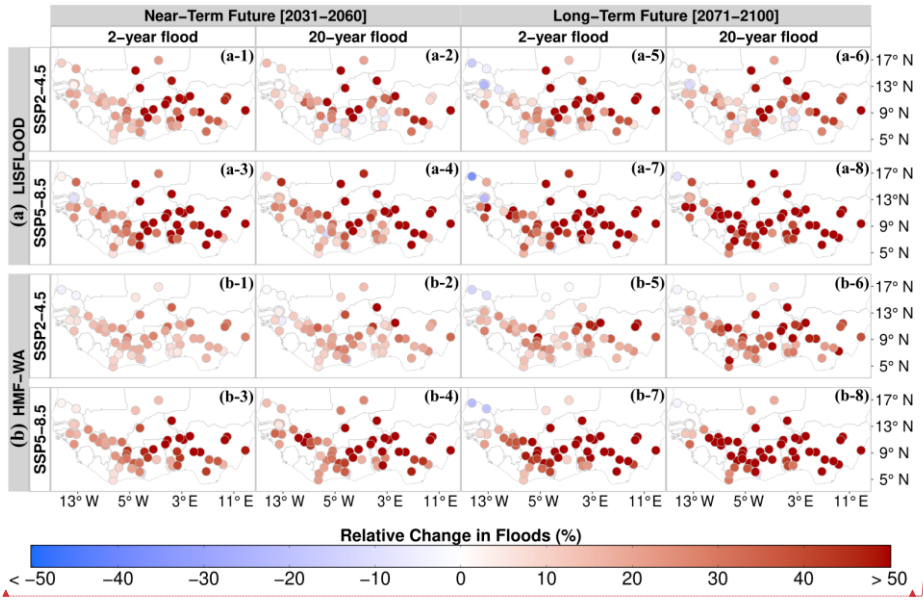

Figure 7: Mean relative changes in the 2-year and 20-year Floods in West Africa for Near-term (2031-2060) and Long-term (2071-2100) futures, based on simulations from the LISFLOOD (a-1 to a-8) and HMF-WA (b-1 to b-8) hydrological models, under SSP2-4.5 and SSP5-8.5 scenarios.

3.3 Onset of changes in AMF series

3.3.1 Observed trends in GEV Parameters

As the climate and environment change (Lee et al., 2023), it is essential to examine how these changes affect the parameters of GEV distributions. Figure 8 shows the spatial distribution of trends detected by the Mann-Kendall test on ~~GEV parameters estimated on multi-model mean streamflow~~ GEV parameters estimated on multi models mean AMF over 30-year moving windows from 1950 to 2100. Both hydrological models project upward trends in the location and scale parameters across the West African region with a strong agreement between the two hydrological models (see Figure 8). All local trends are field significant at 0.05 level according to the FDR procedure. The simulated upward trends in both parameters, observed across various watersheds and emission scenarios, emphasize the importance of accounting for

a mis en forme : Police :11 pt, Gras
a mis en forme : Police :11 pt, Gras
a mis en forme : Police :11 pt, Gras
a mis en forme : Police :11 pt
a mis en forme : Police :11 pt
a mis en forme : Police :11 pt

temporal variability in GEV parameters to reliably model future flood risks. An increase in the location parameter suggests more frequent and severe floods, while an upward trend in the scale parameter indicates greater variability in flood magnitudes. In contrast, the "mixed" trends observed in the shape parameter, with no distinct spatial patterns, support the decision to model it as constant over time, as there is no strong regional evidence of consistent temporal changes in its behaviour across the region.

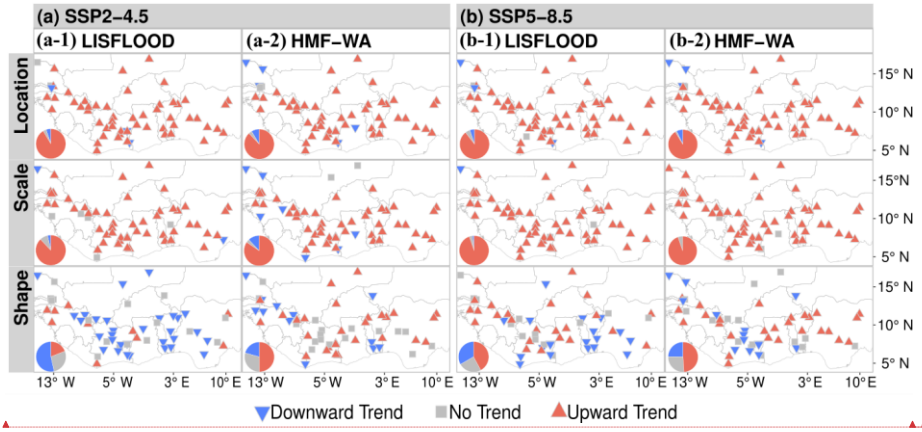

Figure 8: Direction of significant trends detected using the Mann-Kendall trend test (at the 0.05 significance level) for GEV parameters: location (top row), scale (middle row), and shape (bottom row). The GEV parameters are estimated based on multi-model mean streamflow over 30-year moving windows. Panels (a-1) and (b-1) display the results for the LISFLOOD model under SSP2-4.5 and SSP5-8.5, respectively, while panels (a-2) and (b-2) show the results for the HMF-WA model under SSP2-4.5 and SSP5-8.5, respectively. The red upward triangles indicate significant upward trends, and the blue downward triangles indicate significant downward trends, both at the 0.05 significance level. Gray rectangles represent cases where no significant trends are detected. The pie charts summarize the proportion of stations showing significant positive trends (red), significant negative trends (blue), and non-significant trends (gray).

3.3.2 Selection of the best-suited GEV trend model

Using non-stationary GEV models, we analyse temporal shifts in floods by fitting time-dependent GEV parameters to the AMF series from both hydrological model's simulations. To detect the onset of significant trends in flood events, we have allowed any starting year (t0) of a possible trend in the GEV location μ(t) and scale σ(t) parameter between 1970 and 2070. To select the best non-stationary GEV model for each site, we have compared the goodness-of-fit

a mis en forme : Police :11 pt, Gras
a mis en forme : Police :11 pt, Gras
a mis en forme : Police :11 pt, Gras
a mis en forme : Police :11 pt, Gras
a mis en forme : Police :11 pt, Gras
a mis en forme : Police :11 pt, Gras
a mis en forme : Non Exposant/ Indice
a mis en forme : Police :12 pt, Non Gras

of three different time-varying GEV models. The models evaluated are: (1) a linear trend for both the μ(t) and σ(t) parameters without a breakpoint (GEV1); (2) a linear trend for μ(t) and σ(t) starting after a specific breakpoint (GEV2); and (3) linear trends for μ(t) and σ(t) both before and after a breakpoint (GEV3). Figure 9 shows the GEV trend model selected at each station according to the AIC criterion and the deviance test for the LISFLOOD-CMIP6 and HMFWA-CMIP6 simulations under both SSP2-4.5 and SSP-8.5 scenarios. Although both hydrological models project an increase in floods (Figure 5), they simulate slightly different trend patterns across the study area. Considering the LISFLOOD model (Figure 9a), the GEV3 (double linear trend) is constantly best suited at most stations, with a high agreement between the CMIP6 models. For instance, under the SSP2-4.5 scenario, the GEV3 distribution outperforms other models at 66 %, 79 %, 76 %, when the LISFLOOD model is driven by the GFDL (Figure 9a-1), IPSL (Figure 9a-2) and MPI (Figure 9a-3) climate models, respectively. A similar trend is observed under the SSP5-8.5 where the GEV3 is best suited when the LISFLOOD is forced with the MPI (62 %), MRI (77 %), IPSL (78 %), and UKESM (66 %) models (Figure 9a-7, 9a-8, 9a-9 and 9a-10). The HMF-WA simulations show a mixed spatial pattern between the GEV2 and GEV3 models (Figure 9b). For both hydrological models, the single linear trend model (GEV1) is selected at very few stations (less than 5 %). Meanwhile, the stationary behaviour observed at few sites under SSP2-4.5 suggests that certain river basins may experience little to no change in their hydrological extremes under moderate emissions pathways.

a mis en forme : Police :11 pt, Gras

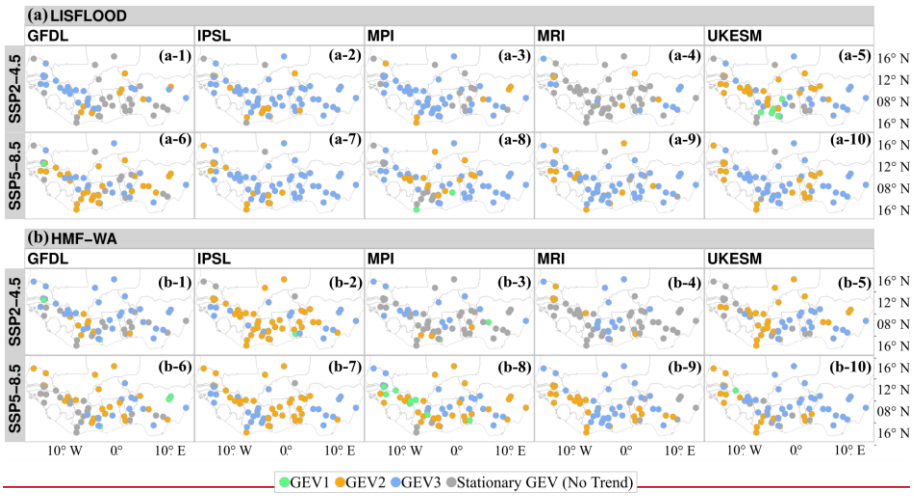

~~Figure 9: Best-fitting GEV trend models at each station, determined using the AIC criterion and the deviance test, based on simulations from (a) LISFLOOD-CMIP6 (top rows) and (b) HMF-WA-CMIP6 (bottom rows) simulations under SSP2-4.5 and SSP5-8.5 scenarios. The green points represent stations best modelled by GEV1, which assumes a linear trend over the entire record. The orange points indicate stations best modelled by GEV2, which assumes stationarity before a breakpoint followed by a linear trend after the breakpoint. The blue points denote stations best modelled by GEV3, which assumes a double linear trend. The grey points represent stations where all non-stationary GEV models are rejected based on the deviance test.~~

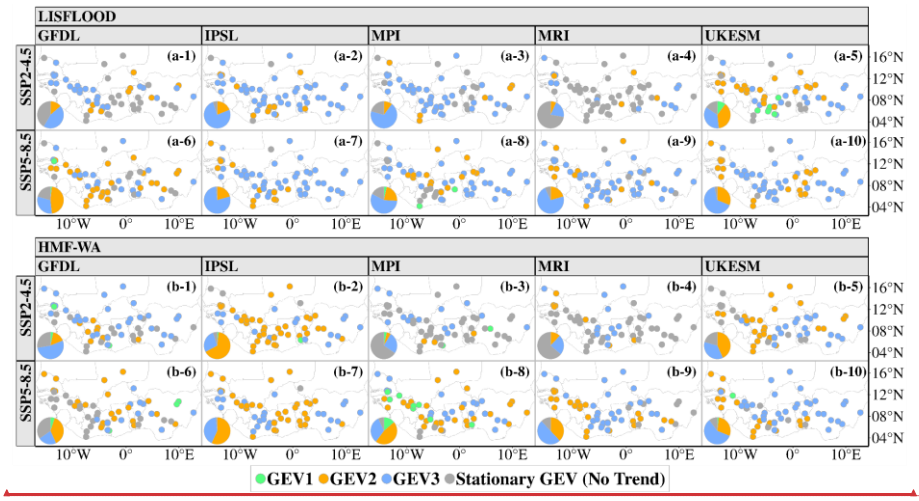

Figure 9: Best-fitting GEV trend models at each station, determined using the AIC criterion and the deviance test, based on simulations from (a) LISFLOOD-CMIP6 (top rows) and (b) HMF-WA-CMIP6 (bottom rows) simulations under SSP2-4.5 and SSP5-8.5 scenarios. The green points represent stations best modelled by GEV1, which assumes a linear trend over the entire record. The orange points indicate stations best modelled by GEV2, which assumes stationarity before a breakpoint followed by a linear trend after the breakpoint. The blue points denote stations best modelled by GEV3, which assumes a double linear trend. The grey points represent stations where all non-stationary GEV models are rejected based on the deviance test. The pie charts summarize the proportion of stations at which the stationary GEV model (grey), or one of the non-stationary models, GEV1 (green), GEV2 (orange), or GEV3 (blue), is identified as the best-suited for fitting the AMF series.

3.3.3 Starting years of trends in flood hazards

a mis en forme : Police :11 pt, Gras

a mis en forme : Police :11 pt, Gras

a mis en forme : Police :11 pt, Gras

a mis en forme : Police :11 pt, Gras

a mis en forme : Interligne : Multiple 1,15 li

The spatial distribution of the starting years of significant flood trends detected with the GEV trend models are shown in Figure 10. The projections from the two hydrological models are spatially coherent, and the temporal variability on the start of flood trends in the region seems to depend on climate models. Overall, under both SSP2-4.5 and SSP5-8.5, the majority of significant trends are identified almost on the whole record, from the 1980s onward, in agreement with long-term trends observed in this region (Tramblay et al., 2020), particularly with the GFDL, IPSL, MPI, and UKESM models. This consistent pattern of early starting years suggests that West African communities are already facing high flood risks, and are likely to experience exacerbated conditions in the near-future. On the two linear trends in the GEV3 model, as shown in Supplementary Figure S5, the predominant spatial pattern is a transition from decreasing flood trends before the breakpoint to increasing trends after. Persistent increases, characterized by positive slopes before and after the breakpoint, are also observed at several sites, particularly with the GFDL, IPSL, and UKESM climate models.

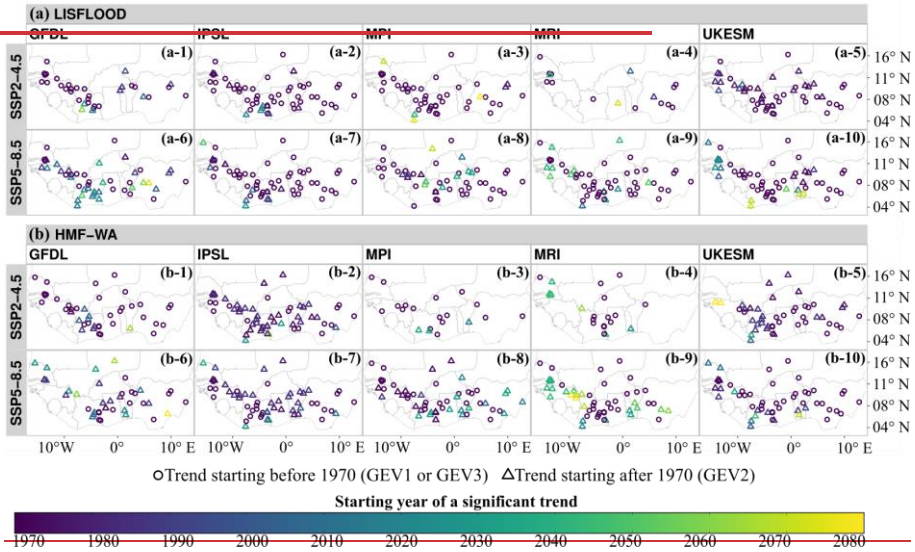

Figure 10: Spatial distribution of the starting years of significant flood trends projected by (a) LISFLOOD and (b) HMF-WA hydrological models, forced with CMIP6 models (GFDL, IPSL, MPI, MRI, and UKESM), under SSP2-4.5 and SSP5-8.5 scenarios. The color gradient indicates the years of significant breakpoints in flood trends, ranging from 1970 (purple) to 2070 (yellow). Circular markers represent sites where trends began at the start of the time series (before 1970). Triangular markers indicate sites where trends emerged after 1970 (the linear trend GEV2 case).

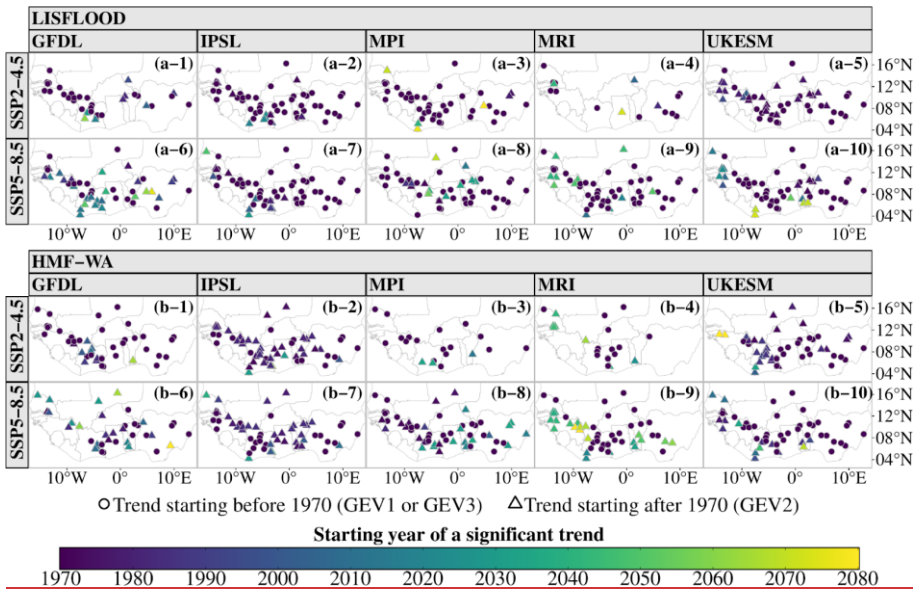

Figure 10: Spatial distribution of the starting years of significant flood trends projected by (a) LISFLOOD and (b) HMF-WA hydrological models, forced with CMIP6 models (GFDL, IPSL,MPI, MRI, and UKESM), under SSP2-4.5 and SSP5-8.5 scenarios. The color gradient indicates the starting year of a significant flood trend, ranging from 1970 (purple) to 2070 (yellow). Circular markers represent sites where trends began at the start of the time series (before 1970). Triangular markers indicate sites where trends emerged after 1970 (the linear trend GEV2 case).

Conclusions

a mis en forme : Police :12 pt, Non Gras

This study has assessed the regional-scale hydrological impacts of climate change in West Africa, specifically focusing on floods, from two large-scale hydrological models (HMF-WA and LISFLOOD) driven by five bias-corrected CMIP6 climate models under SSP2-4.5 and SSP5-8.5 scenarios. A multi-model index of agreement (MIA) was used to assess the robustness of the projections from the hydrological model. The statistical evaluation of the two hydrological models, performed using the two-sample Anderson-Darling test between the annual maximum flows observed from the ADHI database and those simulated by the hydrological models, revealed that the LISFLOOD model outperforms the HMF-WA model in simulating extreme flows in West Africa. The GEV distribution was used to analyse trends and

detect change points by fitting and comparing multiple GEV models to the AMF series, covering both the historical and future periods. Two 30-year future periods (a near-term future [2031–2060] and a long-term future [2071–2100]) were compared to a reference historical period (1985-2014). Despite differences in hydrological processes representation, model architectures and calibration, the two hydrological models generally projected consistent impacts of climate change on future floods across the West African region with a relatively high level of consistency. This agreement between the two hydrological models suggests that the climate forcing has more importance than the hydrological representation itself, and un-calibrated models can provide reliable scenarios in this region. An increase in floods (2-year and 20-year) is observed at more than 94 % of the stations, with some locations experiencing flood magnitudes exceeding 45 %. The results of the comparison between GEV trend models show that the double-linear trend GEV model with both location and scale parameters expressed as time-dependent is the best suited for most stations. The analysis of the starting years of significant flood trends revealed that most shifts in extreme flood patterns occurred early in the time series, as early as the 1970s in several basins.

The use of the GCM outputs to drive hydrological models introduces uncertainties in hydrological simulations. Indeed, the outputs of General Circulation Models (GCMs) are characterised by uncertainties, arising from several factors such as the simplified representation of complex Earth system interactions and atmospheric processes, the uncertain socioeconomic pathways, the coarse spatial resolution of these models, along with challenges related to model parameterization (Hawkins & Sutton, 2009). In addition, the performance of large-scale hydrological models is influenced by the driving inputs, the representation of the hydrological process, and the model parameterization (Andersson et al., 2015). Current models also have difficulties in reproducing hydrological processes in arid regions (Heinicke et al., 2024). It would therefore be interesting to explore in more details the main sources of uncertainties in hydrological projections in West Africa to improve the realism of such modelling approaches in the future.

Code availability

The codes used in this study are available upon request. The implementation of these codes primarily relies on the R extRemes library (https://www.jstatsoft.org/article/view/v072i08).

a mis en forme : Police :12 pt, Non Gras

a mis en forme : Police :12 pt, Non Gras

Data availability

The ADHI dataset containing the observed annual maximum time series is available at: https://doi.org/10.23708/LXGXQ9, and annual maximum dataset from the HMF-WA simulations is available at: https://doi.org/10.5285/346124fd-a0c6-490f-b5af-eaccbb26ab6b. The data that support the findings of this study are available from the corresponding author upon reasonable request.

Author contributions

SBD, YT, and AB conceived and designed the study, with contributions from JE and BD. SBD, YT, and JB developed the methodology. YT provided the ADHI dataset and parametric bootstrapping code to assess the significance of flood trends. JE, BD, SG, and PS carried out the LISFLOOD simulations. PR provided the HMF-WA model annual maximum flow dataset. JB provided R code snippets to implement the GEV trend models. SBD performed the flood frequency analysis and drafted the initial manuscript. YT and AB supervised the study. All authors contributed to the writing and revision of the manuscript.

Competing interest declaration

The authors declare that they have no conflict of interest.

Acknowledgements

The PhD Grant of Serigne Bassirou Diop is funded by the AFD/IRD project CECC. The Phd Grant of Job Ekolu is funded by the Centre for Agroecology Water and Resilience (CAWR) of Coventry University, UK. The authors also extend their thanks to the various basin agencies in West Africa for their contribution to data collection and Nathalie Rouche (SIEREM) for the database management. Yves Tramblay and Bastien Dieppois were supported by a PHC ALLIANCE grant. Juliette Blanchet acknowledges receiving funding from Agence Nationale de la Recherche - France 2030 as part of the PEPR TRACCS programme under grant number ANR-22-EXTR-0005. Ponnambalam Rameshwaran was supported by the Natural Environment Research Council as part of the NC-International program (NE/X006247/1).

a mis en forme : Police :Non Gras

a mis en forme : Police :12 pt, Non Gras

a mis en forme : Police :12 pt, Non Gras

a mis en forme : Police :12 pt

a mis en forme : Police :12 pt, Non Gras

References

Agoungbome, S. M. D., Seidou, O., & Thiam, M. (2018). Evaluation and Update of Two Regional Methods (ORSTOM and CIEH) for Estimations of Flow Used in Structural Design in West Africa. In C. M. F. Kebe, A. Gueye, A. Ndiaye, & A. Garba (Eds.), Innovations and Interdisciplinary Solutions for Underserved Areas (pp. 153–162). Springer International Publishing. https://doi.org/10.1007/978-3-319-98878-8_15

Aich, V., Liersch, S., Vetter, T., Fournet, S., Andersson, J. C. M., Calmanti, S., van Weert, F. H. A., Hattermann, F. F., & Paton, E. N. (2016). Flood projections within the Niger River Basin under future land use and climate change. Science of The Total Environment, 562, 666–677. https://doi.org/10.1016/j.scitotenv.2016.04.021

Akaike, H. (1974). A new look at the statistical model identification. IEEE Transactions on Automatic Control, 19(6), 716–723. https://doi.org/10.1109/TAC.1974.1100705

Almazroui, M., Saeed, F., Saeed, S., Nazrul Islam, M., Ismail, M., Klutse, N. A. B., & Siddiqui, M. H. (2020). Projected Change in Temperature and Precipitation Over Africa from CMIP6. Earth Systems and Environment, 4(3), 455–475. https://doi.org/10.1007/s41748-020-00161-x

Andersson, J., Pechlivanidis, I., Gustafsson, D., Donnelly, C., & Arheimer, B. (2015). Key factors for improving large-scale hydrological model performance. European Water, 49, 77–88.

Arnell, N. W., & Gosling, S. N. (2016). The impacts of climate change on river flood risk at the global scale. Climatic Change, 134(3), 387–401. https://doi.org/10.1007/s10584-014-1084-5

Awotwi, A., Annor, T., Anornu, G. K., Quaye-Ballard, J. A., Agyekum, J., Ampadu, B., Nti, I. K., Gyampo, M. A., & Boakye, E. (2021). Climate change impact on streamflow in a tropical basin of Ghana, West Africa. Journal of Hydrology: Regional Studies, 34, 100805. https://doi.org/10.1016/j.ejrh.2021.100805

Babaousmail, H., Ayugi, B. O., Ojara, M., Ngoma, H., Oduro, C., Mumo, R., & Ongoma, V. (2023). Evaluation of CMIP6 models for simulations of diurnal temperature range over Africa. Journal of African Earth Sciences, 202, 104944. https://doi.org/10.1016/j.jafrearsci.2023.104944

Bell, V. A., Kay, A. L., Jones, R. G., & Moore, R. J. (2007). Development of a high resolution grid-based river flow model for use with regional climate model output. Hydrology and Earth System Sciences, 11(1), 532–549. https://doi.org/10.5194/hess-11-532-2007

Berger, V. W., & Zhou, Y. (2014). Kolmogorov–Smirnov Test: Overview. In R. S. Kenett, N. T. Longford, W. W. Piegorsch, & F. Ruggeri (Eds.), Wiley StatsRef: Statistics Reference Online (1st ed.). Wiley. https://doi.org/10.1002/9781118445112.stat06558

Biaou, S., Gouwakinnou, G. N., Noulèkoun, F., Salako, K. V., Houndjo Kpoviwanou, J. M. R., Houehanou, T. D., & Biaou, H. S. S. (2023). Incorporating intraspecific variation into species distribution models improves climate change analyses of a widespread West African tree species (Pterocarpus erinaceus Poir, Fabaceae). Global Ecology and Conservation, 45, e02538. https://doi.org/10.1016/j.gecco.2023.e02538

Bichet, A., Diedhiou, A., Hingray, B., Evin, G., Touré, N. E., Browne, K. N. A., & Kouadio, K. (2020). Assessing uncertainties in the regional projections of precipitation in CORDEX-AFRICA. Climatic Change, 162(2), 583–601. https://doi.org/10.1007/s10584-020-02833-z

Blanchet, J., Molinié, G., & Touati, J. (2018). Spatial analysis of trend in extreme daily rainfall in southern France. Climate Dynamics, 51(3), 799–812. https://doi.org/10.1007/s00382-016-3122-7

Bodian, A., Dezetter, A., Deme, A., & Diop, L. (2016). Hydrological Evaluation of TRMM Rainfall over the Upper Senegal River Basin. Hydrology, 3(2), 15. https://doi.org/10.3390/hydrology3020015

a mis en forme : Police :12 pt, Non Gras

a mis en forme : Police :Non Italique

a mis en forme : Police :Non Gras

a mis en forme : Police :Non Italique, Français (France)

a mis en forme : Français (France)

a mis en forme : Police :Non Italique, Français (France)

a mis en forme : Français (France)

a mis en forme : Police :Non Gras, Français (France)

a mis en forme : Police :Non Gras, Français (France)

a mis en forme : Police :Non Gras

Bodian, A., Dezetter, A., Diop, L., Deme, A., Djaman, K., & Diop, A. (2018). Future Climate Change Impacts on Streamflows of Two Main West Africa River Basins: Senegal and Gambia. Hydrology, 5(1), 21. https://doi.org/10.3390/hydrology5010021

Bodian, A., Diop, L., Panthou, G., Dacosta, H., Deme, A., Dezetter, A., Ndiaye, P. M., Diouf, I., & Vischel, T. (2020). Recent Trend in Hydroclimatic Conditions in the Senegal River Basin. Water, 12(2), Article 2. https://doi.org/10.3390/w12020436

Bruneau, P., Gascuel-Odoux, C., Robin, P., Merot, Ph., & Beven, K. (1995). Sensitivity to space and time resolution of a hydrological model using digital elevation data. Hydrological Processes, 9(1), 69–81. https://doi.org/10.1002/hyp.3360090107

Brunner, M. I., Slater, L., Tallaksen, L. M., & Clark, M. (2021). Challenges in modeling and predicting floods and droughts: A review. WIREs Water, 8(3), e1520. https://doi.org/10.1002/wat2.1520

Calton, B., Schellekens, J., & Martinez-de la Torre, A. (2016). Water Resource Reanalysis v1: Data Access and Model Verification Results (Version v1.02) [Computer software]. Zenodo. https://doi.org/10.5281/zenodo.57760

Chagnaud, G., Panthou, G., Vischel, T., & Lebel, T. (2023). Capturing and Attributing the Rainfall Regime Intensification in the West African Sahel with CMIP6 Models. Journal of Climate, 36(6), 1823–1843. https://doi.org/10.1175/jcli-d-22-0412.1

Chagnaud, G., Panthou, G., Vischel, T., & Lebel, T. (2022). A synthetic view of rainfall intensification in the West African Sahel. Environmental Research Letters, 17(4), 044005. https://doi.org/10.1088/1748-9326/ac4a9c

Choulga, M., Moschini, F., Mazzetti, C., Grimaldi, S., Disperati, J., Beck, H., Salamon, P., & Prudhomme, C. (2024). Technical note: Surface fields for global environmental modelling. Hydrology and Earth System Sciences, 28(13), 2991–3036. https://doi.org/10.5194/hess-28-2991-2024

Chu, H., Lin, Y., Huang, C., Hsu, C., & Chen, H. (2010). Modelling the hydrologic effects of dynamic land-use change using a distributed hydrologic model and a spatial land-use allocation model. Hydrological Processes, 24(18), 2538–2554. https://doi.org/10.1002/hyp.7667

Coles, S. (2001). An introduction to statistical modeling of extreme values. Springer.

CRED. (2022). 2021 Disasters in numbers. Brussels: CRED. https://www.cred.be/sites/default/files/2021_EMDAT_report.pdf

Cunderlik, J. (2003). Hydrologic Model Selection for the CFCAS Project: Assessment of Water Resources Risk and Vulnerability to Changing Climatic Conditions. Water Resources Research Report. https://ir.lib.uwo.ca/wrrr/9

Davie, J. C. S., Falloon, P. D., Kahana, R., Dankers, R., Betts, R., Portmann, F. T., Wisser, D., Clark, D. B., Ito, A., Masaki, Y., Nishina, K., Fekete, B., Tessler, Z., Wada, Y., Liu, X., Tang, Q., Hagemann, S., Stacke, T., Pavlick, R., … Arnell, N. (2013). Comparing projections of future changes in runoff from hydrological and biome models in ISI-MIP. Earth System Dynamics, 4(2), 359–374. https://doi.org/10.5194/esd-4-359-2013

Dawson, C. W., Abrahart, R. J., Shamseldin, A. Y., Wilby, R. L., & See, L. M. (2005). Neural network modelling of the 20-year flood event for catchments across the UK. Proceedings. 2005 IEEE International Joint Conference on Neural Networks, 2005., 4, 2637–2642. https://doi.org/10.1109/IJCNN.2005.1556319

De Longueville, F., Ozer, P., Gemenne, F., Henry, S., Mertz, O., & Nielsen, J. Ø. (2020). Comparing climate change perceptions and meteorological data in rural West Africa to improve the understanding of household decisions to migrate. Climatic Change, 160(1), 123–141. https://doi.org/10.1007/s10584-020-02704-7

Dee, D. P., Uppala, S. M., Simmons, A. J., Berrisford, P., Poli, P., Kobayashi, S., Andrae, U., Balmaseda, M. A., Balsamo, G., Bauer, P., Bechtold, P., Beljaars, A. C. M., van de Berg, L.,

a mis en forme : Police :Non Italique, Français (France)

a mis en forme : Français (France)

a mis en forme : Police :Non Italique, Français (France)

a mis en forme : Français (France)

a mis en forme : Police :Non Gras, Français (France)

a mis en forme : Police :Non Gras, Français (France)

a mis en forme : Français (France)

a mis en forme : Police :Non Gras

Bidlot, J., Bormann, N., Delsol, C., Dragani, R., Fuentes, M., Geer, A. J., … Vitart, F. (2011). The ERA-Interim reanalysis: Configuration and performance of the data assimilation system. Quarterly Journal of the Royal Meteorological Society, 137(656), 553–597. https://doi.org/10.1002/qj.828

Descroix, L., Guichard, F., Grippa, M., Lambert, L. A., Panthou, G., Mahé, G., Gal, L., Dardel, C., Quantin, G., Kergoat, L., Bouaïta, Y., Hiernaux, P., Vischel, T., Pellarin, T., Faty, B., Wilcox, C., Malam Abdou, M., Mamadou, I., Vandervaere, J.-P., ... Paturel, J.-E. (2018). Evolution of Surface Hydrology in the Sahelo-Sudanian Strip: An Updated Review. Water, 10(6), 748. https://doi.org/10.3390/w10060748

Diallo, A., Donkor, E., & Owusu, V. (2020). Climate change adaptation strategies, productivity and sustainable food security in southern Mali. Climatic Change, 159(3), 309–327. https://doi.org/10.1007/s10584-020-02684-8

Diop S.B., Tramblay Y., Bodian A., Ekolu J., Rouché N., Dieppois B., 2025. Flood frequency analysis in West Africa, Journal of Flood Risk Management, 18: e70001. https://doi.org/10.1111/jfr3.70001

Dosio, A., Jones, R. G., Jack, C., Lennard, C., Nikulin, G., & Hewitson, B. (2019). What can we know about future precipitation in Africa? Robustness, significance and added value of projections from a large ensemble of regional climate models. Climate Dynamics, 53(9), 5833–5858. https://doi.org/10.1007/s00382-019-04900-3

Dosio, A., Jury, M. W., Almazroui, M., Ashfaq, M., Diallo, I., Engelbrecht, F. A., Klutse, N. A. B., Lennard, C., Pinto, I., Sylla, M. B., & Tamoffo, A. T. (2021). Projected future daily characteristics of African precipitation based on global (CMIP5, CMIP6) and regional (CORDEX, CORDEX-CORE) climate models. Climate Dynamics, 57(11), 3135–3158. https://doi.org/10.1007/s00382-021-05859-w

Dotse, S.-Q., Larbi, I., Limantol, A. M., Asare-Nuamah, P., Frimpong, L. K., Alhassan, A.-R. M., Sarpong, S., Angmor, E., & Ayisi-Addo, A. K. (2023). Rainfall Projections from Coupled Model Intercomparison Project Phase 6 in the Volta River Basin: Implications on Achieving Sustainable Development. Sustainability, 15(2), Article 2. https://doi.org/10.3390/su15021472

ECOWREX. (2018). Ecowas Observatory For Renewable Energy And Energy Efficiency Projects. Projects http://www.ecowrex.org/resources/projects

Ehret, U., Zehe, E., Wulfmeyer, V., Warrach-Sagi, K., & Liebert, J. (2012). HESS Opinions "Should we apply bias correction to global and regional climate model data?" Hydrology and Earth System Sciences, 16(9), 3391–3404. https://doi.org/10.5194/hess-16-3391-2012

Ekolu, J., Dieppois, B., Diop, S. B., Bodian, A., Grimaldi, S., Salamon, P., Villarini, G., Eden, J. M., Monerie, P.-A., van de Wiel, M., & Tramblay, Y. (2025). How could climate change affect the magnitude, duration and frequency of hydrological droughts and floods in West Africa during the 21st century? A storyline approach. Journal of Hydrology, 627, 133482. https://doi.org/10.1016/j.jhydrol.2025.133482

Ekolu, J., Dieppois, B., Tramblay, Y., Villarini, G., Slater, L. J., Mahé, G., Paturel, J.-E., Eden, J. M., Moulds, S., Sidibe, M., Camberlin, P., Pohl, B., & van de Wiel, M. (2024). Variability in flood frequency in sub-Saharan Africa: The role of large-scale climate modes of variability and their future impacts. Journal of Hydrology, 640, 131679. https://doi.org/10.1016/j.jhydrol.2024.131679

El Adlouni, S., Ouarda, T. B. M. J., Zhang, X., Roy, R., & Bobée, B. (2007). Generalized maximum likelihood estimators for the nonstationary generalized extreme value model. Water Resources Research, 43(3). https://doi.org/10.1029/2005WR004545

Elagib, N. A., Zayed, I. S. A., Saad, S. A. G., Mahmood, M. I., Basheer, M., & Fink, A. H. (2021). Debilitating floods in the Sahel are becoming frequent. Journal of Hydrology, 599, 126362.

a mis en forme : Police :Non Gras

https://doi.org/10.1016/j.jhydrol.2021.126362
EM-DAT. (2015). The OFDA/CRED International Disaster Database. Centre for Research on the Epidemiology of Disasters (CRED). Université catholique de Louvain. http://www.emdat.be
Engmann, S., & Cousineau, D. (2011). Comparing distributions: The two-sample Anderson–Darling test as an alternative to the Kolmogorov–Smirnov test. Journal of Applied Quantitative Methods, 6, 1–17.
Famien, A. M., Janicot, S., Ochou, A. D., Vrac, M., Defrance, D., Sultan, B., & Noël, T. (2018). A bias-corrected CMIP5 dataset for Africa using the CDF-t method – a contribution to agricultural impact studies. Earth System Dynamics, 9(1), 313–338. https://doi.org/10.5194/esd-9-313-2018
Farris, S., Deidda, R., Viola, F., & Mascaro, G. (2021). On the Role of Serial Correlation and Field Significance in Detecting Changes in Extreme Precipitation Frequency. Water Resources Research, 57(11), e2021WR030172. https://doi.org/10.1029/2021WR030172
Feaster, T. D., Gotvald, A. J., Musser, J. W., Weaver, J. C., Kolb, K., Veilleux, A. G., & Wagner, D. M. (2023). Magnitude and frequency of floods for rural streams in Georgia, South Carolina, and North Carolina, 2017—Results. In Scientific Investigations Report (2023–5006). U.S. Geological Survey. https://doi.org/10.3133/sir20235006
Fisher, R. A. (1992). Statistical Methods for Research Workers. In S. Kotz & N. L. Johnson (Eds.), Breakthroughs in Statistics: Methodology and Distribution (pp. 66–70). Springer. https://doi.org/10.1007/978-1-4612-4380-9_6
Flaounas, E., Drobinski, P., Vrac, M., Bastin, S., Lebeaupin-Brossier, C., Stéfanon, M., Borga, M., & Calvet, J.-C. (2013). Precipitation and temperature space–time variability and extremes in the Mediterranean region: Evaluation of dynamical and statistical downscaling methods. Climate Dynamics, 40(11), 2687–2705. https://doi.org/10.1007/s00382-012-1558-y
Fortin, F.-A., De Rainville, F.-M., Gardner, M.-A. G., Parizeau, M., & Gagné, C. (2012). DEAP: Evolutionary algorithms made easy. J. Mach. Learn. Res., 13(1), 2171–2175.
Fréchet, M. (1927). Sur la loi de probabilité de l'écart maximum. Annales de la Société Polonaise de Mathématique. 6.
Frieler, K., Lange, S., Piontek, F., Reyer, C. P. O., Schewe, J., Warszawski, L., Zhao, F., Chini, L., Denvil, S., Emanuel, K., Geiger, T., Halladay, K., Hurtt, G., Mengel, M., Murakami, D., Ostberg, S., Popp, A., Riva, R., Stevanovic, M., … Yamagata, Y. (2017). Assessing the impacts of 1.5 °C global warming – simulation protocol of the Inter-Sectoral Impact Model Intercomparison Project (ISIMIP2b). Geoscientific Model Development, 10(12), 4321–4345. https://doi.org/10.5194/gmd-10-4321-2017
Gebremeskel, S., Liu, Y. B., De Smedt, F., Hoffmann, L., & Pfister, L. (2005). Assessing the hydrological effects of Landuse changes using distributed hydrological modelling and GIS. International Journal of River Basin Management, 3(4), 261–271. https://doi.org/10.1080/15715124.2005.9635266
Gosling, S. N., Zaherpour, J., Mount, N. J., Hattermann, F. F., Dankers, R., Arheimer, B., Breuer, L., Ding, J., Haddeland, I., Kumar, R., Kundu, D., Liu, J., Van Griensven, A., Veldkamp, T. I. E., Vetter, T., Wang, X., & Zhang, X. (2017). A comparison of changes in river runoff from multiple global and catchment-scale hydrological models under global warming scenarios of 1 °C, 2 °C and 3 °C. Climatic Change, 141(3), 577–595. https://doi.org/10.1007/s10584-016-1773-3
Gudmundsson, L., Wagener, T., Tallaksen, L. M., & Engeland, K. (2012). Evaluation of nine large-scale hydrological models with respect to the seasonal runoff climatology in Europe. Water Resources Research, 48(11). https://doi.org/10.1029/2011WR010911
Gumbel, E. J. (1958). Statistics of Extremes. Columbia University Press.

a mis en forme : Police :Non Italique

https://doi.org/10.7312/gumb92958
Gupta, H. V., Kling, H., Yilmaz, K. K., & Martinez, G. F. (2009). Decomposition of the mean squared error and NSE performance criteria: Implications for improving hydrological modelling. Journal of Hydrology, 377(1), 80–91. https://doi.org/10.1016/j.jhydrol.2009.08.003
Haddeland, I., Matheussen, B. V., & Lettenmaier, D. P. (2002). Influence of spatial resolution on simulated streamflow in a macroscale hydrologic model. Water Resources Research, 38(7). https://doi.org/10.1029/2001WR000854
Hamdi, Y., Duluc, C.-M., & Rebour, V. (2018). Temperature Extremes: Estimation of Non-Stationary Return Levels and Associated Uncertainties. Atmosphere, 9(4), Article 4. https://doi.org/10.3390/atmos9040129
Hamed, K. H., & Rao, A. R. (1998). A modified Mann-Kendall trend test for autocorrelated data. Journal of Hydrology, 204, 182–196. https://doi.org/10.1016/S0022-1694(97)00125-X
Han, X., Mehrotra, R., Sharma, A., & Rahman, A. (2022). Incorporating nonstationarity in regional flood frequency analysis procedures to account for climate change impact. Journal of Hydrology, 612, 128235. https://doi.org/10.1016/j.jhydrol.2022.128235
Hansen, J., Ruedy, R., Sato, M., & Lo, K. (2010). GLOBAL SURFACE TEMPERATURE CHANGE. Reviews of Geophysics, 48(4). https://doi.org/10.1029/2010RG000345
Hawkins, E., & Sutton, R. (2009). The Potential to Narrow Uncertainty in Regional Climate Predictions. Bulletin of the American Meteorological Society, 90(8), 1095–1108. https://doi.org/10.1175/2009BAMS2607.1
Hawkins, E., & Sutton, R. (2012). Time of emergence of climate signals. Geophysical Research Letters, 39(1). https://doi.org/10.1029/2011GL050087
Heinicke, S., Volkholz, J., Schewe, J., Gosling, S. N., Schmied, H. M., Zimmermann, S., Mengel, M., Sauer, I. J., Burek, P., Chang, J., Kou-Giesbrecht, S., Grillakis, M., Guillaumot, L., Hanasaki, N., Koutroulis, A., Otta, K., Qi, W., Satoh, Y., Stacke, T., … Frieler, K. (2024). Global hydrological models continue to overestimate river discharge. Environmental Research Letters, 19(7), 074005. https://doi.org/10.1088/1748-9326/ad52b0
Hersbach, H., Bell, B., Berrisford, P., Hirahara, S., Horányi, A., Muñoz-Sabater, J., Nicolas, J., Peubey, C., Radu, R., Schepers, D., Simmons, A., Soci, C., Abdalla, S., Abellan, X., Balsamo, G., Bechtold, P., Biavati, G., Bidlot, J., Bonavita, M., De Chiara, G., Dahlgren, P., Dee, D., Diamantakis, M., Dragani, R., Flemming, J., Forbes, R., Fuentes, M., Geer, A., Haimberger, L., Healy, S., Hogan, R. J., Hólm, E., Janisková, M., Keeley, S., Laloyaux, P., Lopez, P., Lupu, C., Radnoti, G., de Rosnay, P., Rozum, I., Vamborg, F., Villaume, S., & Thépaut, J.-N. (2020). The ERA5 global reanalysis. Quarterly Journal of the Royal Meteorological Society, 146(730), 1999–2049. https://doi.org/10.1002/qj.3803
Hochberg, Y., & Benjamini, Y. (1995). Controlling the false discovery rate: A practical and powerful approach to multiple testing. JR Stat Soc, 57(1), 289–300.
Hosking, J. R. M. (1990). L-Moments: Analysis and Estimation of Distributions Using Linear Combinations of Order Statistics. Journal of the Royal Statistical Society: Series B (Methodological), 52(1), 105–124. https://doi.org/10.1111/j.2517-6161.1990.tb01775.x
Hossain, A., Mathias, C., & Blanton, R. (2021). Remote Sensing of Turbidity in the Tennessee River Using Landsat 8 Satellite. Remote Sensing, 2021, 3785. https://doi.org/10.3390/rs13183785
Houghton, J. E. T., Ding, Y., Griggs, D., Noguer, M., van der Linden, P., Dai, X., Maskell, M., & Johnson, C. (2001). Climate Change 2001: The Scientific Basis. In Contribution of Working Group I to the Third Assessment Report of the Intergovernmental Panel on Climate Change (IPCC): Vol. 881. (p. 881).
Huang, X., Yin, J., Slater, L. J., Kang, S., He, S., & Liu, P. (2024). Global Projection of Flood Risk With a Bivariate Framework Under 1.5–3.0°C Warming Levels. Earth's Future, 12(4),

e2023EF004312. https://doi.org/10.1029/2023EF004312
IPCC. (2021). Sixth Assessment Report (AR6): Climate Change 2021: The Physical Science Basis. Cambridge University Press.
Jajarmizad, M., Harun, S., & Salarpour, M. (2012). A Review on Theoretical Consideration and Types of Models in Hydrology. Journal of Environmental Science and Technology, 5(5), 249–261. https://doi.org/10.3923/jest.2012.249.261
Jayaweera, L., Wasko, C., & Nathan, R. (2024). Modelling non-stationarity in extreme rainfall using large-scale climate drivers. Journal of Hydrology, 636, 131309. https://doi.org/10.1016/j.jhydrol.2024.131309
Katz, R. W. (2013). Statistical Methods for Nonstationary Extremes. In A. AghaKouchak, D. Easterling, K. Hsu, S. Schubert, & S. Sorooshian (Eds.), Extremes in a Changing Climate: Detection, Analysis and Uncertainty (pp. 15–37). Springer Netherlands. https://doi.org/10.1007/978-94-007-4479-0_2
Kauffeldt, A., Halldin, S., Rodhe, A., Xu, C.-Y., & Westerberg, I. K. (2013). Disinformative data in large-scale hydrological modelling. Hydrology and Earth System Sciences, 17(7), 2845–2857. https://doi.org/10.5194/hess-17-2845-2013
Kendall, M. G. (1975). Rank correlation methods (4th ed., 2d impression). Griffin London.
Khaliq, M. N., Ouarda, T. B. M. J., Gachon, P., Sushama, L., & St-Hilaire, A. (2009). Identification of hydrological trends in the presence of serial and cross correlations: A review of selected methods and their application to annual flow regimes of Canadian rivers. Journal of Hydrology, 368(1), 117–130. https://doi.org/10.1016/j.jhydrol.2009.01.035
Klutse, N. A. B., Quagraine, K. A., Nkrumah, F., Quagraine, K. T., Berkoh-Oforiwaa, R., Dzrobi, J. F., & Sylla, M. B. (2021). The Climatic Analysis of Summer Monsoon Extreme Precipitation Events over West Africa in CMIP6 Simulations. Earth Systems and Environment, 5(1), 25–41. https://doi.org/10.1007/s41748-021-00203-y
Koubodana, H. D., Atchonouglo, K., Adounkpe, J. G., Amoussou, E., Kodja, D. J., Koungbanane, D., Afoudji, K. Y., Lombo, Y., & Kpemoua, K. E. (2021). Surface runoff prediction and comparison using IHACRES and GR4J lumped models in the Mono catchment, West Africa. Proceedings of the International Association of Hydrological Sciences, 384, 63–68. https://doi.org/10.5194/piahs-384-63-2021
Krishnamurthy, P. K., Lewis, K., & Choularton, R. K. (2012). Climate impacts on food security and nutrition—A review of existing knowledge. Met Office and WFP's Office for Climate Change, Environment and Disaster Risk Reduction: Exeter, UK.
Kwakye, S. O., & Bárdossy, A. (2020). Hydrological modelling in data-scarce catchments: Black Volta basin in West Africa. SN Applied Sciences, 2(4), 628. https://doi.org/10.1007/s42452-020-2454-4
Lalou, R., Sultan, B., Muller, B., & Ndonky, A. (2019). Does climate opportunity facilitate smallholder farmers' adaptive capacity in the Sahel? Palgrave Communications, 5(1), 1–11. https://doi.org/10.1057/s41599-019-0288-8
Land, V. van der, Romankiewicz, C., & Geest, K. van der. (2018). Environmental change and migration: A review of West African case studies. In Routledge Handbook of Environmental Displacement and Migration. Routledge.
Lange, S. (2018). Bias correction of surface downwelling longwave and shortwave radiation for the EWEMBI dataset. Earth System Dynamics, 9(2), 627–645. https://doi.org/10.5194/esd-9-627-2018
Lange, S. (2019). EartH2Observe, WFDEI and ERA-Interim data Merged and Bias-corrected for ISIMIP (EWEMBI) (Version 1.1, p. 1 Files) [Application/octet-stream]. GFZ Data Services. https://doi.org/10.5880/PIK.2019.004

Lawrence, D. (2020). Uncertainty introduced by flood frequency analysis in projections for changes in flood magnitudes under a future climate in Norway. Journal of Hydrology: Regional Studies, 28, 100675. https://doi.org/10.1016/j.ejrh.2020.100675

Lee, H., Calvin, K., Dasgupta, D., Krinner, G., Mukherji, A., Thorne, P., Trisos, C., Romero, J., Aldunce, P., Barret, K., & others. (2023). IPCC, 2023: Climate Change 2023: Synthesis Report, Summary for Policymakers. Contribution of Working Groups I, II and III to the Sixth Assessment Report of the Intergovernmental Panel on Climate Change [Core Writing Team, H. Lee and J. Romero (eds.)]. IPCC, Geneva, Switzerland.

Mann, H. B. (1945). Nonparametric Tests Against Trend. Econometrica, 13(3), 245. https://doi.org/10.2307/1907187

Martins, E. S., & Stedinger, J. R. (2000). Generalized maximum-likelihood generalized extreme-value quantile estimators for hydrologic data. Water Resources Research, 36(3), 737–744. https://doi.org/10.1029/1999WR900330

Masson-Delmotte, V. P., Zhai, P., Pirani, S. L., Connors, C., Péan, S., Berger, N., Caud, Y., Chen, L., Goldfarb, M. I., & Scheel Monteiro, P. M. (2021). IPCC, 2021: Summary for Policymakers. In: Climate Change 2021: The Physical Science Basis. Contribution of Working Group I to the Sixth Assessment Report of the Intergovernmental Panel on Climate Change [Report]. Cambridge University Press, Cambridge, United Kingdom and New York, NY, USA. https://researchspace.csir.co.za/dspace/handle/10204/12710

Matthew, O. A., Owolabi, O. A., Osabohien, R., Urhie, E., Ogunbiyi, T., Olawande, T. I., Edafe, O. D., & Daramola, P. J. (2020). Carbon Emissions, Agricultural Output and Life Expectancy in West Africa. International Journal of Energy Economics and Policy, 10(3), Article 3.

Michelangeli, P.-A., Vrac, M., & Loukos, H. (2009). Probabilistic downscaling approaches: Application to wind cumulative distribution functions. Geophysical Research Letters, 36(11). https://doi.org/10.1029/2009GL038401

Monerie, P.-A., Dittus, A. J., Wilcox, L. J., & Turner, A. G. (2023). Uncertainty in Simulating Twentieth Century West African Precipitation Trends: The Role of Anthropogenic Aerosol Emissions. Earth's Future, 11(2), e2022EF002995. https://doi.org/10.1029/2022EF002995

Mudge, J. F., Baker, L. F., Edge, C. B., & Houlahan, J. E. (2012). Setting an Optimal α That Minimizes Errors in Null Hypothesis Significance Tests. PLOS ONE, 7(2), e32734. https://doi.org/10.1371/journal.pone.0032734

Muñoz-Sabater, J., Dutra, E., Agustí-Panareda, A., Albergel, C., Arduini, G., Balsamo, G., Boussetta, S., Choulga, M., Harrigan, S., Hersbach, H., Martens, B., Miralles, D. G., Piles, M., Rodríguez-Fernández, N. J., Zsoter, E., Buontempo, C., & Thépaut, J.-N. (2021). ERA5-Land: A state-of-the-art global reanalysis dataset for land applications. Earth System Science Data, 13(9), 4349–4383. https://doi.org/10.5194/essd-13-4349-2021

Ndehedehe, C. E. (2019). The water resources of tropical West Africa: Problems, progress, and prospects. Acta Geophysica, 67(2), 621–649. https://doi.org/10.1007/s11600-019-00260-y

Nicholson, S. E. (2018). Climate of the Sahel and West Africa. In S. E. Nicholson, Oxford Research Encyclopedia of Climate Science. Oxford University Press. https://doi.org/10.1093/acrefore/9780190228620.013.510

Niel, H., Paturel, J.-E., & Servat, E. (2003). Study of parameter stability of a lumped hydrologic model in a context of climatic variability. Journal of Hydrology, 278(1–4), 213–230. https://doi.org/10.1016/S0022-1694(03)00158-6

Nka, B. N., Oudin, L., Karambiri, H., Paturel, J. E., & Ribstein, P. (2015). Trends in floods in West Africa: Analysis based on 11 catchments in the region. Hydrology and Earth System Sciences, 19(11), 4707–4719. https://doi.org/10.5194/hess-19-4707-2015

Noël, T., Loukos, H., Defrance, D., Vrac, M., & Levavasseur, G. (2022). Extending the global high-

resolution downscaled projections dataset to include CMIP6 projections at increased resolution coherent with the ERA5-Land reanalysis. Data in Brief, 45, 108669. https://doi.org/10.1016/j.dib.2022.108669

Nooni, I. K., Ogou, F. K., Chaibou, A. A. S., Nakoty, F. M., Gnitou, G. T., & Lu, J. (2023). Evaluating CMIP6 Historical Mean Precipitation over Africa and the Arabian Peninsula against Satellite-Based Observation. Atmosphere, 14(3), Article 3. https://doi.org/10.3390/atmos14030607

O'Neill, B. C., Kriegler, E., Ebi, K. L., Kemp-Benedict, E., Riahi, K., Rothman, D. S., van Ruijven, B. J., van Vuuren, D. P., Birkmann, J., Kok, K., Levy, M., & Solecki, W. (2017). The roads ahead: Narratives for shared socioeconomic pathways describing world futures in the 21st century. Global Environmental Change, 42, 169–180. https://doi.org/10.1016/j.gloenvcha.2015.01.004

Orange, D. (1990). Hydroclimatologie du Fouta Djalon et dynamique actuelle d'un vieux paysage latéritique (Afrique de l'Ouest).

Panthou, G., Vischel, T., Lebel, T., Quantin, G., Pugin, A.-C. F., Blanchet, J., & Ali, A. (2013). From pointwise testing to a regional vision: An integrated statistical approach to detect nonstationarity in extreme daily rainfall. Application to the Sahelian region. Journal of Geophysical Research: Atmospheres, 118(15), 8222–8237. https://doi.org/10.1002/jgrd.50340

Papalexiou, S. M., & Koutsoyiannis, D. (2013). Battle of extreme value distributions: A global survey on extreme daily rainfall. Water Resources Research, 49(1), 187–201. https://doi.org/10.1029/2012WR012557

Pechlivanidis, I. G., Arheimer, B., Donnelly, C., Hundecha, Y., Huang, S., Aich, V., Samaniego, L., Eisner, S., & Shi, P. (2017). Analysis of hydrological extremes at different hydro-climatic regimes under present and future conditions. Climatic Change, 141(3), 467–481. https://doi.org/10.1007/s10584-016-1723-0

Pielke, R., & Ritchie, J. (2021). How Climate Scenarios Lost Touch With Reality. Issues in Science and Technology, 37(4), 74–83.

Pierce, D. W., Cayan, D. R., Maurer, E. P., Abatzoglou, J. T., & Hegewisch, K. C. (2015). Improved Bias Correction Techniques for Hydrological Simulations of Climate Change. Journal of Hydrometeorology, 16(6), 2421–2442. https://doi.org/10.1175/JHM-D-14-0236.1

Pokhrel, P., Gupta, H. V., & Wagener, T. (2008). A spatial regularization approach to parameter estimation for a distributed watershed model. Water Resources Research, 44(12), 2007WR006615. https://doi.org/10.1029/2007WR006615

Pospichal, B., Karam, D. B., Crewell, S., Flamant, C., Hünerbein, A., Bock, O., & Saïd, F. (2010). Diurnal cycle of the intertropical discontinuity over West Africa analysed by remote sensing and mesoscale modelling. Quarterly Journal of the Royal Meteorological Society, 136(S1), 92. https://doi.org/10.1002/qj.435

Prosdocimi, I., & Kjeldsen, T. (2021). Parametrisation of change-permitting extreme value models and its impact on the description of change. Stochastic Environmental Research and Risk Assessment, 35(2), 307–324. https://doi.org/10.1007/s00477-020-01940-8

Prudhomme, C., Zsótér, E., Matthews, G., Melet, A., Grimaldi, S., Zuo, H., Hansford, E., Harrigan, S., Mazzetti, C., de Boisseson, E., Salamon, P., & Garric, G. (2024). Global hydrological reanalyses: The value of river discharge information for world-wide downstream applications – The example of the Global Flood Awareness System GloFAS. Meteorological Applications, 31(2), e2192. https://doi.org/10.1002/met.2192

Rai, S., Hoffman, A., Lahiri, S., Nychka, D. W., Sain, S. R., & Bandyopadhyay, S. (2024). Fast parameter estimation of generalized extreme value distribution using neural networks. Environmetrics, 35(3), e2845. https://doi.org/10.1002/env.2845

Rameshwaran, P., Bell, V. A., Brown, M. J., Davies, H. N., Kay, A. L., Rudd, A. C., & Sefton, C. (2022). Use of Abstraction and Discharge Data to Improve the Performance of a National-Scale

Hydrological Model. Water Resources Research, 58(1), e2021WR029787. https://doi.org/10.1029/2021WR029787

Rameshwaran, P., Bell, V. A., Davies, H. N., & Kay, A. L. (2021). How might climate change affect river flows across West Africa? Climatic Change, 169(3), 21. https://doi.org/10.1007/s10584-021-03256-0

Reed, S., Koren, V., Smith, M., Zhang, Z., Moreda, F., Seo, D.-J., & Dmip Participants, A. (2004). Overall distributed model intercomparison project results. Journal of Hydrology, 298(1–4), 27–60. https://doi.org/10.1016/j.jhydrol.2004.03.031

Riahi, K., van Vuuren, D. P., Kriegler, E., Edmonds, J., O'Neill, B. C., Fujimori, S., Bauer, N., Calvin, K., Dellink, R., Fricko, O., Lutz, W., Popp, A., Cuaresma, J. C., Kc, S., Leimbach, M., Jiang, L., Kram, T., Rao, S., Emmerling, J., … Tavoni, M. (2017). The Shared Socioeconomic Pathways and their energy, land use, and greenhouse gas emissions implications: An overview. Global Environmental Change, 42, 153–168. https://doi.org/10.1016/j.gloenvcha.2016.05.009

Rodríguez-Fonseca, B., Mohino, E., Mechoso, C. R., Caminade, C., Biasutti, M., Gaetani, M., Garcia-Serrano, J., Vizy, E. K., Cook, K., Xue, Y., Polo, I., Losada, T., Druyan, L., Fontaine, B., Bader, J., Doblas-Reyes, F. J., Goddard, L., Janicot, S., Arribas, A., … Voldoire, A. (2015). Variability and Predictability of West African Droughts: A Review on the Role of Sea Surface Temperature Anomalies. Journal of Climate, 28(10), 4034–4060. https://doi.org/10.1175/JCLI-D-14-00130.1

Roudier, P., Sultan, B., Quirion, P., & Berg, A. (2011). The impact of future climate change on West African crop yields: What does the recent literature say? Global Environmental Change, 21(3), 1073–1083. https://doi.org/10.1016/j.gloenvcha.2011.04.007

Salamon, P., Grimaldi, S., Disperati, J., Prudhomme, C., Choulga, M., Moschini, F., & Mazzetti, C. (2023). LISFLOOD static and parameter maps for GloFAS. European Commission, JRC132801.

Santer, B. D., Bonfils, C. J. W., Fu, Q., Fyfe, J. C., Hegerl, G. C., Mears, C., Painter, J. F., Po-Chedley, S., Wentz, F. J., Zelinka, M. D., & Zou, C.-Z. (2019). Celebrating the anniversary of three key events in climate change science. Nature Climate Change, 9(3), 180–182. https://doi.org/10.1038/s41558-019-0424-x

Sauer, I. J., Reese, R., Otto, C., Geiger, T., Willner, S. N., Guillod, B. P., Bresch, D. N., & Frieler, K. (2021). Climate signals in river flood damages emerge under sound regional disaggregation. Nature Communications, 12(1), 2128. https://doi.org/10.1038/s41467-021-22153-9

Scholz, F. W., & Stephens, M. A. (1986). K-Sample Anderson-Darling Tests of Fit, for Continuous and Discrete Cases, Technical Report. University of Washington, Seattle.

Sillmann, J., Kharin, V. V., Zhang, X., Zwiers, F. W., & Bronaugh, D. (2013). Climate extremes indices in the CMIP5 multimodel ensemble: Part 1. Model evaluation in the present climate. Journal of Geophysical Research: Atmospheres, 118(4), 1716–1733. https://doi.org/10.1002/jgrd.50203

Song, J.-H., Her, Y., & Kang, M.-S. (2022). Estimating Reservoir Inflow and Outflow From Water Level Observations Using Expert Knowledge: Dealing With an Ill-Posed Water Balance Equation in Reservoir Management. Water Resources Research, 58(4), e2020WR028183. https://doi.org/10.1029/2020WR028183

Srivast, A. K., Rahimi, J., Alsafadi, K., Vianna, M., Enders, A., Zheng, W., Demircan, A., Dieng, M. D. B., Salack, S., Faye, B., Singh, M., Ewert, F., & Gaiser, T. (2023). Dynamic Modelling of Mixed Crop-Livestock Systems: A Case Study of Climate Change Impacts in sub-Saharan Africa. https://doi.org/10.21203/rs.3.rs-3793846/v1

Stackhouse Jr., P. W., Gupta, S. K., Cox, S. J., Mikovitz, C., Zhang, T., & Hinkelman, L. M. (2011). The NASA/GEWEX Surface Radiation Budget Release 3.0: 24.5-year dataset. Gewex News, 21, 10–12.

Stedinger, J. R., & Griffis, V. W. (2011). Getting From Here to Where? Flood Frequency Analysis and Climate. JAWRA Journal of the American Water Resources Association, 47(3), 506–513. https://doi.org/10.1111/j.1752-1688.2011.00545.x

Sule, I. M., & Odekunle, M. O. (2016). Landscapes of West Africa: A Window on a Changing World. CILLS: Landscapes of West Africa: A Window on a Changing World. US ….

Sultan, B., & Gaetani, M. (2016). Agriculture in West Africa in the Twenty-First Century: Climate Change and Impacts Scenarios, and Potential for Adaptation. Frontiers in Plant Science, 7. https://doi.org/10.3389/fpls.2016.01262

Tang, Q., Oki, T., Kanae, S., & Hu, H. (2007). The Influence of Precipitation Variability and Partial Irrigation within Grid Cells on a Hydrological Simulation. Journal of Hydrometeorology, 8(3), 499–512. https://doi.org/10.1175/JHM589.1

Taylor, C. M., Belušić, D., Guichard, F., Parker, D. J., Vischel, T., Bock, O., Harris, P. P., Janicot, S., Klein, C., & Panthou, G. (2017). Frequency of extreme Sahelian storms tripled since 1982 in satellite observations. Nature, 544 (7651), 475–478). https://doi.org/10.1038/nature22069

Tarpanelli, A., Paris, A., Sichangi, A. W., O`Loughlin, F., & Papa, F. (2023). Water Resources in Africa: The Role of Earth Observation Data and Hydrodynamic Modeling to Derive River Discharge. Surveys in Geophysics, 44(1), 97–122. https://doi.org/10.1007/s10712-022-09744-x

Tian, C., Huang, G., Lu, C., Song, T., Wu, Y., & Duan, R. (2023). Northward Shifts of the Sahara Desert in Response to Twenty-First-Century Climate Change. Journal of Climate, 36(10), 3417–3435. https://doi.org/10.1175/JCLI-D-22-0169.1

Thielen, J., Bartholmes, J., Ramos, M.-H., & De Roo, A. (2009). The European Flood Alert System – Part 1: Concept and development. Hydrology and Earth System Sciences, 13(2), 125–140. https://doi.org/10.5194/hess-13-125-2009

Totin, E., Padgham, J., Ayivor, J., Dietrich, K., Fosu-Mensah, B., Gordon, C., Habtezion, S., Tweneboah Lawson, E., Mensah, A., Nukpezah, D., Ofori, B., Piltz, S., Sidibé, A., Sissoko, M., Traore, P., Dazé, A., & Echeverría, D. (2016). Vulnerability and Adaptation to Climate Change in Semi-Arid Areas in West Africa. https://doi.org/10.13140/RG.2.2.15263.87202

Tramblay Y., Villarini G., Wei Z., 2020. Observed changes in flood hazard in Africa. Environmental Research Letters, 15, 1040b5, https://doi.org/10.1088/1748-9326/abb90b

Tramblay, Y., El Khalki, E. M., Khedimallah, A., Sadaoui, M., Benaabidate, L., Boulmaiz, T., Boutaghane, H., Dakhlaoui, H., Hanich, L., Ludwig, W., Meddi, M., Elmehdi Saidi, M., & Mahé, G. (2024). Regional flood frequency analysis in North Africa. Journal of Hydrology, 630, 130678. https://doi.org/10.1016/j.jhydrol.2024.130678

Tramblay, Y., Rouché, N., Paturel, J.-E., Mahé, G., Boyer, J.-F., Amoussou, E., Bodian, A., Dacosta, H., Dakhlaoui, H., Dezetter, A., Hughes, D., Hanich, L., Peugeot, C., Tshimanga, R., & Lachassagne, P. (2021). ADHI: The African Database of Hydrometric Indices (1950–2018). Earth System Science Data, 13(4), 1547–1560. https://doi.org/10.5194/essd-13-1547-2021

Tramblay, Y., & Somot, S. (2018). Future evolution of extreme precipitation in the Mediterranean. Climatic Change, 151(2), 289–302. https://doi.org/10.1007/s10584-018-2300-5

Tran, Q. Q., De Niel, J., & Willems, P. (2018). Spatially Distributed Conceptual Hydrological Model Building: A Generic Top-Down Approach Starting From Lumped Models. Water Resources Research, 54(10), 8064–8085. https://doi.org/10.1029/2018WR023566

UNDRR. (2023). Annual Report 2023. United Nations Office for Disaster Risk Reduction.

UNEP. (2020). Water Scarcity in Sub-Saharan Africa. United Nations Environment Programme.

Van Der Knijff, J. M., Younis, J., & De Roo, A. P. J. (2010). LISFLOOD: A GIS-based distributed model for river basin scale water balance and flood simulation. International Journal of

Geographical Information Science, 24(2), 189–212. https://doi.org/10.1080/13658810802549154

Vintrou, E. (2012). Cartographie et caractérisation des systèmes agricoles au Mali par télédétection à moyenne résolution spatiale [PhD Thesis]. AgroParisTech.

Weedon, G. P., Balsamo, G., Bellouin, N., Gomes, S., Best, M. J., & Viterbo, P. (2014). The WFDEI meteorological forcing data set: WATCH Forcing Data methodology applied to ERA-Interim reanalysis data. Water Resources Research, 50(9), 7505–7514. https://doi.org/10.1002/2014WR015638

Weibull, W. (1951). A Statistical Distribution Function of Wide Applicability. Journal of Applied Mechanics, 18(3), 293–297. https://doi.org/10.1115/1.4010337

Wasko, C., Westra, S., Nathan, R., Orr, H. G., Villarini, G., Villalobos Herrera, R., & Fowler, H. J. (2021). Incorporating climate change in flood estimation guidance. Philosophical Transactions of the Royal Society A: Mathematical, Physical and Engineering Sciences, 379(2195), 20190548. https://doi.org/10.1098/rsta.2019.0548

Wilcox, C., Vischel, T., Panthou, G., Bodian, A., Blanchet, J., Descroix, L., Quantin, G., Cassé, C., Tanimoun, B., & Kone, S. (2018). Trends in hydrological extremes in the Senegal and Niger Rivers. Journal of Hydrology, 566, 531–545. https://doi.org/10.1016/j.jhydrol.2018.07.063

Wilks, D. S. (2006). On "Field Significance" and the False Discovery Rate. Journal of Applied Meteorology and Climatology, 45(9), 1181–1189. https://doi.org/10.1175/JAM2404.1

Wilks, D. S. (2016). "The Stippling Shows Statistically Significant Grid Points": How Research Results are Routinely Overstated and Overinterpreted, and What to Do about It. Bulletin of the American Meteorological Society, 97(12), 2263–2273. https://doi.org/10.1175/BAMS-D-15-00267.1

Wilson, C. B., Valdes, J. B., & Rodriguez-Iturbe, I. (1979). On the influence of the spatial distribution of rainfall on storm runoff. Water Resources Research, 15(2), 321–328. https://doi.org/10.1029/WR015i002p00321

Wolock, D. M., & Price, C. V. (1994). Effects of digital elevation model map scale and data resolution on a topography-based watershed model. Water Resources Research, 30(11), 3041–3052. https://doi.org/10.1029/94WR01971

World Bank. (2021a). An EPIC response: Innovative governance for Flood and Drought Risk Management. World Bank.

World Bank. (2021b). World Bank Engagement in Transboundary Waters in West Africa: Retrospective and Lessons Learned. World Bank, Washington, DC.

Zhao, F., Nie, N., Liu, Y., Yi, C., Guillaumot, L., Wada, Y., Burek, P., Smilovic, M., Frieler, K., Buechner, M., Schewe, J., & Gosling, S. N. (2025). Benefits of Calibrating a Global Hydrological Model for Regional Analyses of Flood and Drought Projections: A Case Study of the Yangtze River Basin. Water Resources Research, 61(3), e2024WR037153. https://doi.org/10.1029/2024WR037153